Hadron Spectroscopy at the COMPASS Experiment

Boris Grube
for the COMPASS Collaboration

Physik-Department E18
Technische Universität München,
Garching, Germany

Kernphysikalisches Kolloquium
HISKP Bonn, 05. June 2014

Outline

1. Introduction
   - QCD and the constituent quark model
   - Beyond the constituent quark model
2. How to measure meson spectra?
   - Meson production in diffractive dissociation
   - Partial-wave analysis method
3. Selected results
   - Partial-wave decomposition of the $(3\pi)^-$ final state
   - Resonance extraction in the $\pi^-\pi^+\pi^-$ system
4. Conclusions and outlook

Outline

1. Introduction
   - QCD and the constituent quark model
   - Beyond the constituent quark model
2. How to measure meson spectra?
   - Meson production in diffractive dissociation
   - Partial-wave analysis method
3. Selected results
   - Partial-wave decomposition of the $(3\pi)^-$ final state
   - Resonance extraction in the $\pi^-\pi^+\pi^-$ system
4. Conclusions and outlook

Hadrons and the Theory of Strong Interaction

- Hadrons are made out of quarks and gluons
- Quantum chromodynamics (QCD) describes interaction of quark and gluon fields
  - Non-abelian gauge theory: gluons carry charge and self-interact

Phenomenon of *confinement*

- Quarks and gluons *do not* exist outside of hadrons
- Only composites reach detector

Hadrons and the Theory of Strong Interaction

- Hadrons are made out of quarks and gluons
- Quantum chromodynamics (QCD) describes interaction of quark and gluon fields
  - Non-abelian gauge theory: gluons carry charge and self-interact

Phenomenon of *confinement*

- Quarks and gluons *do not* exist outside of hadrons
- Only composites reach detector

Hadrons and the Theory of Strong Interaction

Confinement still not understood

- One of 10 physics problems for the next millennium
  "Can we quantitatively understand quark and gluon confinement in Quantum Chromodynamics and the existence of a mass gap?"

  Strings 2000, Int. J. Mod. Phys. **A16** (2001) 1012

- One of seven \$1 000 000 Millenium Prize Problems
  "Yang-Mills existence and mass gap" Clay Mathematics Institute
- Closely related to hadron masses
  - Only $\approx 2\%$ of proton mass explained by Higgs mechanism
  - 98% generated dynamically

Hadrons reflect workings of QCD at low energies

Measurement of **hadron spectra** and **hadron decays** gives valuable input to theory and phenomenology

Hadrons and the Theory of Strong Interaction

Confinement still not understood

- One of 10 physics problems for the next millennium

  "Can we quantitatively understand quark and gluon confinement in Quantum Chromodynamics and the existence of a mass gap?"

  Strings 2000, Int. J. Mod. Phys. **A16** (2001) 1012

- One of seven \$1 000 000 Millenium Prize Problems

  "Yang-Mills existence and mass gap" Clay Mathematics Institute

- Closely related to hadron masses
  - Only $\approx$ 2% of proton mass explained by Higgs mechanism
  - 98% generated dynamically

Hadrons reflect workings of QCD at low energies

Measurement of **hadron spectra** and **hadron decays** gives valuable input to theory and phenomenology

Mesons in the Constituent Quark Model (CQM)

Mesons

- Color-singlet $|q\bar{q}'\rangle$ states, grouped into $\mathrm{SU}(N)_{\mathrm{flavor}}$ multiplets

Spin-parity rules for bound $q\bar{q}$ system

- **Forbidden J^{PC}: $0^{--}, 0^{+-}, 1^{-+}, 2^{+-}, 3^{-+}, \ldots$**
- Extension to charged mesons via G parity: $G = C\,(-1)^I$
  - I isospin of meson
  - Convention: assign J^{PC} quantum numbers of neutral partner state

Mesons in the Constituent Quark Model (CQM)

Mesons

- Color-singlet $|q\bar{q}'\rangle$ states, grouped into $\mathrm{SU}(N)_{\mathrm{flavor}}$ multiplets

Spin-parity rules for bound $q\bar{q}$ system

- Quark spins couple to total intrinsic spin $S = 0$ or 1
- Relative orbital angular Momentum $\vec{L}$ and total spin $\vec{S}$ couple to meson spin $\vec{J} = \vec{L} + \vec{S}$

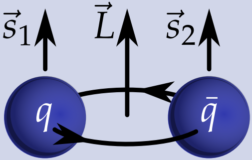

- Parity $P = (-1)^{L+1}$
- Charge conjugation $C = (-1)^{L+S}$
- **Forbidden J^{PC}: $0^{--}, 0^{+-}, 1^{-+}, 2^{+-}, 3^{-+}, \ldots$**
- Extension to charged mesons via G parity: $G = C\,(-1)^I$
  - I isospin of meson
  - *Convention:* assign J^{PC} quantum numbers of neutral partner state

Mesons in the Constituent Quark Model (CQM)

Mesons

- Color-singlet $|q\bar{q}'\rangle$ states, grouped into $\mathrm{SU}(N)_{\mathrm{flavor}}$ multiplets

Spin-parity rules for bound $q\bar{q}$ system

- Quark spins couple to total intrinsic spin $S = 0$ or 1
- Relative orbital angular Momentum $\vec{L}$ and total spin $\vec{S}$ couple to meson spin $\vec{J} = \vec{L} + \vec{S}$
- Parity $P = (-1)^{L+1}$
- Charge conjugation $C = (-1)^{L+S}$
- **Forbidden J^{PC}: $0^{--}, 0^{+-}, 1^{-+}, 2^{+-}, 3^{-+}, \ldots$**
- Extension to charged mesons via G parity: $G = C\,(-1)^I$
  - I isospin of meson
  - *Convention:* assign J^{PC} quantum numbers of neutral partner state

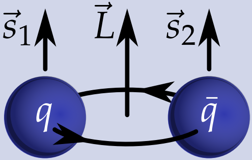

Mesons in the Constituent Quark Model (CQM)

Mesons

- Color-singlet $|q\bar{q}'\rangle$ states, grouped into $\mathrm{SU}(N)_{\text{flavor}}$ multiplets

Spin-parity rules for bound $q\bar{q}$ system

- Quark spins couple to total intrinsic spin $S = 0$ or 1
- Relative orbital angular Momentum $\vec{L}$ and total spin $\vec{S}$ couple to meson spin $\vec{J} = \vec{L} + \vec{S}$

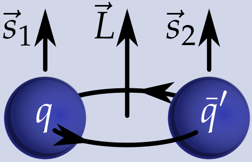

- Parity $P = (-1)^{L+1}$
- Charge conjugation $C = (-1)^{L+S}$
- **Forbidden J^{PC}: $0^{--}, 0^{+-}, 1^{-+}, 2^{+-}, 3^{-+}, \ldots$**
- Extension to charged mesons via G parity: $G = C\,(-1)^I$
  - I isospin of meson
  - *Convention:* assign J^{PC} quantum numbers of neutral partner state

Quark-Model SU(3)$_{\text{flavor}}$ Meson Nonets

Light-quark mesons

- u, d, and s quarks $\Longrightarrow$ SU(3)$_{\text{flavor}}$ nonets

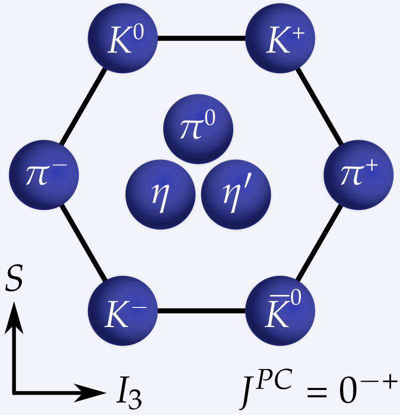

$J^{PC} = 0^{-+}$

Quark-Model SU(3)$_{\text{flavor}}$ Meson Nonets

Light-quark mesons

- u, d, and s quarks $\Longrightarrow$ SU(3)$_{\text{flavor}}$ nonets

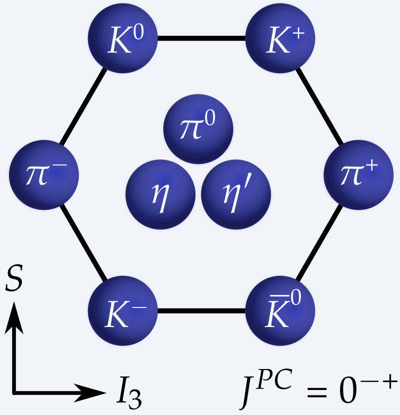

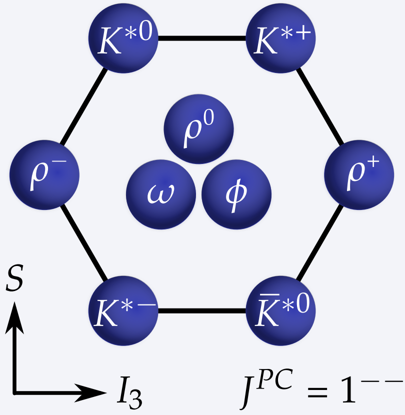

Constituent Quark Model

Light-quark Meson Spectrum

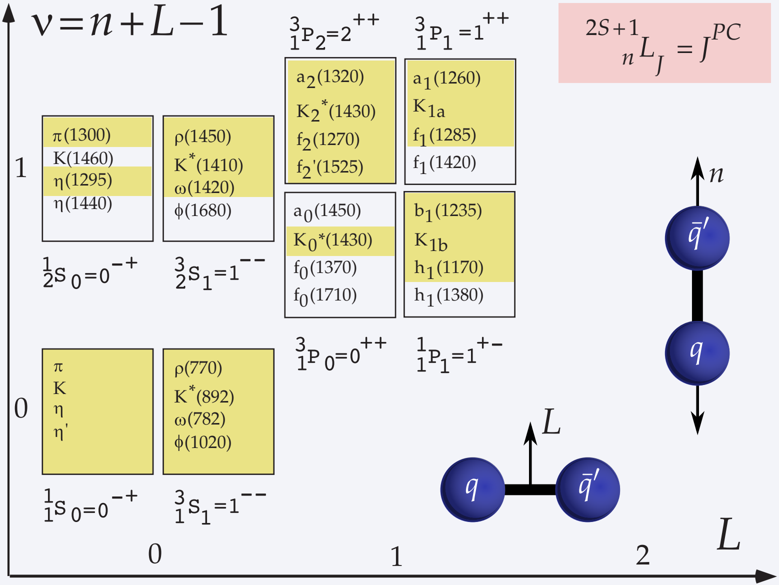

Amsler *et al.*, Phys. Rept. **389** (2004) 61

Constituent Quark Model

Light-quark Meson Spectrum

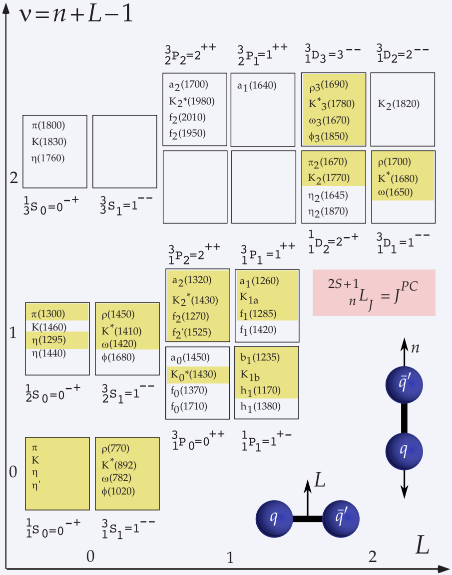

Amsler *et al.*, Phys. Rept. **389** (2004) 61

"Light-meson frontier"

- Many missing and disputed states in mass region $m \approx 2\ \mathrm{GeV}/c^2$
- Identification of higher excitations becomes exceedingly difficult
  - Wider states + higher state density
  - More overlap and mixing

Constituent Quark Model

Light-quark Meson Spectrum

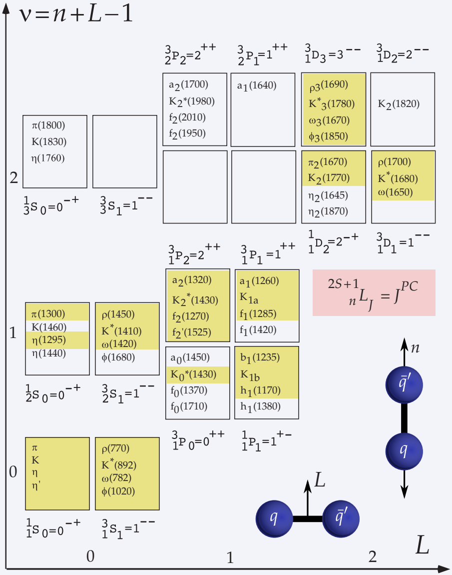

Amsler *et al.*, Phys. Rept. **389** (2004) 61

"Light-meson frontier"

- Many missing and disputed states in mass region $m \approx 2\ \mathrm{GeV}/c^2$
- Identification of higher excitations becomes exceedingly difficult
  - Wider states + higher state density
  - More overlap and mixing

Beyond the Constituent Quark Model

QCD: Gluonic field should manifest itself in hadron spectra

Hybrids $|q\bar{q}g\rangle$

- Resonances with excited gluonic fields
- Glue component contributes to quantum numbers
  - *All* J^{PC} allowed
- Lightest predicted hybrid: spin-exotic $J^{PC} = 1^{-+}$
  - Mass $1.3 \ldots 2.2$ GeV/c^2
  - Experimental candidates $\pi_1(1400)$ and $\pi_1(1600)$ controversial

Glueballs $|gg\rangle$

- Bound states with no valence quarks
- Lightest predicted glueball: ordinary $J^{PC} = 0^{++}$
  - Will strongly mix with nearby conventional $J^{PC} = 0^{++}$ states
  - Mass $1.5 \ldots 2.0$ GeV/c^2
  - Experimental candidate $f_0(1500)$; glueball interpretation disputed

Beyond the Constituent Quark Model

QCD: Gluonic field should manifest itself in hadron spectra

Hybrids $|q\bar{q}g\rangle$

- Resonances with excited gluonic fields
- Glue component contributes to quantum numbers
  - *All* J^{PC} allowed
- Lightest predicted hybrid: spin-exotic $J^{PC} = 1^{-+}$
  - Mass $1.3 \ldots 2.2\ \mathrm{GeV}/c^2$
  - Experimental candidates $\pi_1(1400)$ and $\pi_1(1600)$ controversial

Glueballs $|gg\rangle$

- Bound states with no valence quarks
- Lightest predicted glueball: ordinary $J^{PC} = 0^{++}$
  - Will strongly mix with nearby conventional $J^{PC} = 0^{++}$ states
  - Mass $1.5 \ldots 2.0\ \mathrm{GeV}/c^2$
  - Experimental candidate $f_0(1500)$; glueball interpretation disputed

Beyond the Constituent Quark Model

QCD: Gluonic field should manifest itself in hadron spectra

Hybrids $|q\bar{q}g\rangle$

- Resonances with excited gluonic fields
- Glue component contributes to quantum numbers
  - *All* J^{PC} allowed
- Lightest predicted hybrid: spin-exotic $J^{PC} = 1^{-+}$
  - Mass $1.3 \ldots 2.2$ GeV/c^2
  - Experimental candidates $\pi_1(1400)$ and $\pi_1(1600)$ controversial

Glueballs $|gg\rangle$

- Bound states with no valence quarks
- Lightest predicted glueball: ordinary $J^{PC} = 0^{++}$
  - Will strongly mix with nearby conventional $J^{PC} = 0^{++}$ states
  - Mass $1.5 \ldots 2.0$ GeV/c^2
  - Experimental candidate $f_0(1500)$; glueball interpretation disputed

Beyond the Constituent Quark Model

QCD: Gluonic field should manifest itself in hadron spectra

Hybrids $|q\bar{q}g\rangle$

- Resonances with excited gluonic fields
- Glue component contributes to quantum numbers
  - *All* J^{PC} allowed
- Lightest predicted hybrid: spin-exotic $J^{PC} = 1^{-+}$
  - Mass $1.3 \ldots 2.2$ GeV/c^2
  - Experimental candidates $\pi_1(1400)$ and $\pi_1(1600)$ controversial

Glueballs $|gg\rangle$

- Bound states with no valence quarks
- Lightest predicted glueball: ordinary $J^{PC} = 0^{++}$
  - Will strongly mix with nearby conventional $J^{PC} = 0^{++}$ states
  - Mass $1.5 \ldots 2.0$ GeV/c^2
  - Experimental candidate $f_0(1500)$; glueball interpretation disputed

Beyond the Constituent Quark Model

QCD: Gluonic field should manifest itself in hadron spectra

Hybrids $|q\bar{q}g\rangle$

- Resonances with excited gluonic fields
- Glue component contributes to quantum numbers
  - *All* J^{PC} allowed
- Lightest predicted hybrid: spin-exotic $J^{PC} = 1^{-+}$
  - Mass $1.3 \ldots 2.2\ \text{GeV}/c^2$
  - Experimental candidates $\pi_1(1400)$ and $\pi_1(1600)$ controversial

Glueballs $|gg\rangle$

- Bound states with no valence quarks
- Lightest predicted glueball: ordinary $J^{PC} = 0^{++}$
  - Will strongly mix with nearby conventional $J^{PC} = 0^{++}$ states
  - Mass $1.5 \ldots 2.0\ \text{GeV}/c^2$
  - Experimental candidate $f_0(1500)$; glueball interpretation disputed

Beyond the Constituent Quark Model

QCD in the confinement regime: $\alpha_s = \mathcal{O}(1)$

- QCD Lagrangian *not* calculable using perturbation theory

***Frist-principles* numerical method: Lattice QCD**

- Simulation of QCD on finite discreet space-time lattice using Monte Carlo techniques
- *Challenge:* extrapolation to physical point
  - Heavier u and d quarks than in reality
    $\Longrightarrow$ extrapolation to physical quark masses
  - Extrapolation to infinite volume $L \to \infty$
  - Extrapolation to zero lattice spacing $a \to 0$
    - Rotational symmetry broken due to cubic lattice
- Tremendous progress in past years
  - Finer lattices: spin-identified spectra
  - Larger operator bases: many excited states
  - Access to gluonic content of calculated states

Beyond the Constituent Quark Model

QCD in the confinement regime: $\alpha_s = \mathcal{O}(1)$

- QCD Lagrangian *not* calculable using perturbation theory

Frist-principles numerical method: Lattice QCD

- Simulation of QCD on finite discreet space-time lattice using Monte Carlo techniques
- *Challenge:* extrapolation to physical point
  - Heavier u and d quarks than in reality
    $\Longrightarrow$ extrapolation to physical quark masses
  - Extrapolation to infinite volume $L \to \infty$
  - Extrapolation to zero lattice spacing $a \to 0$
    - Rotational symmetry broken due to cubic lattice
- Tremendous progress in past years
  - Finer lattices: spin-identified spectra
  - Larger operator bases: many excited states
  - Access to gluonic content of calculated states

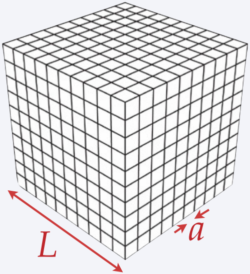

Beyond the Constituent Quark Model

QCD in the confinement regime: $\alpha_s = \mathcal{O}(1)$

- QCD Lagrangian *not* calculable using perturbation theory

***Frist-principles* numerical method: Lattice QCD**

- Simulation of QCD on finite discreet space-time lattice using Monte Carlo techniques
- *Challenge:* extrapolation to physical point
  - Heavier u and d quarks than in reality
    $\Longrightarrow$ extrapolation to physical quark masses
  - Extrapolation to infinite volume $L \to \infty$
  - Extrapolation to zero lattice spacing $a \to 0$
    - Rotational symmetry broken due to cubic lattice
- Tremendous progress in past years
  - Finer lattices: spin-identified spectra
  - Larger operator bases: many excited states
  - Access to gluonic content of calculated states

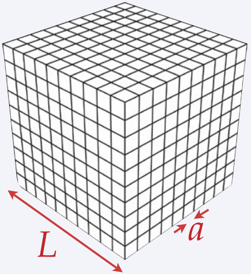

Beyond the Constituent Quark Model

QCD in the confinement regime: $\alpha_s = \mathcal{O}(1)$

- QCD Lagrangian *not* calculable using perturbation theory

***Frist-principles* numerical method: Lattice QCD**

- Simulation of QCD on finite discreet space-time lattice using Monte Carlo techniques
- *Challenge:* extrapolation to physical point
  - Heavier u and d quarks than in reality
    $\Longrightarrow$ extrapolation to physical quark masses
  - Extrapolation to infinite volume $L \to \infty$
  - Extrapolation to zero lattice spacing $a \to 0$
    - Rotational symmetry broken due to cubic lattice
- Tremendous progress in past years
  - Finer lattices: spin-identified spectra
  - Larger operator bases: many excited states
  - Access to gluonic content of calculated states

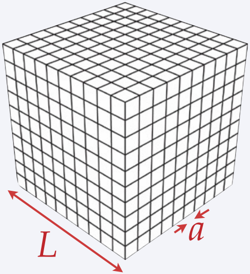

Light-Meson Spectrum in Lattice QCD

State-of-the-art $I = 1$ spectrum

Dudek *et al.*, *arXiv:1309.2608*

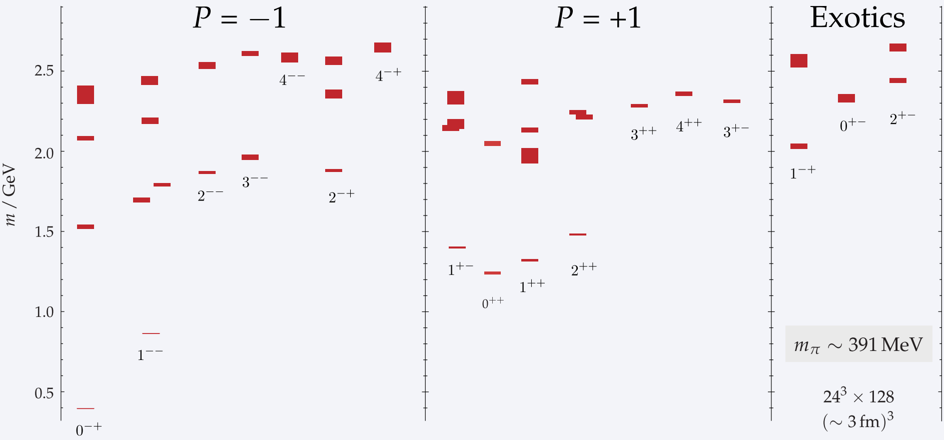

Light-Meson Spectrum in Lattice QCD

State-of-the-art $I = 1$ spectrum

Dudek *et al.*, *arXiv:1309.2608*

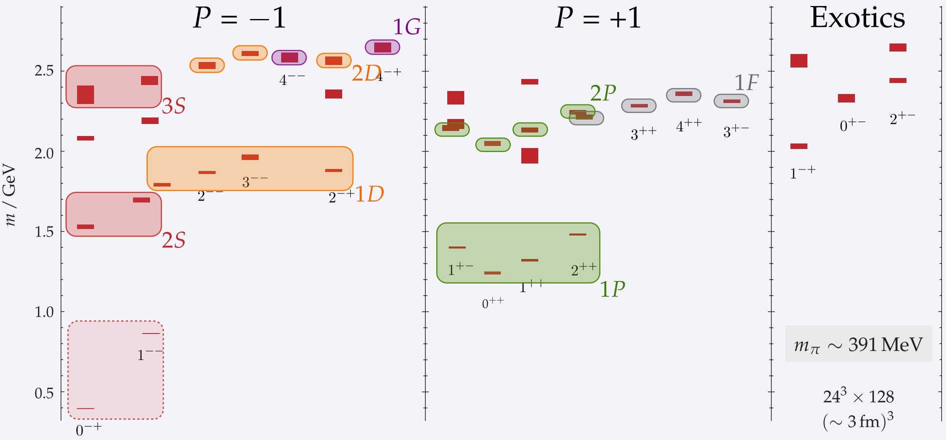

- Near-degeneracy patterns: $q\bar{q}$ super-multiplets

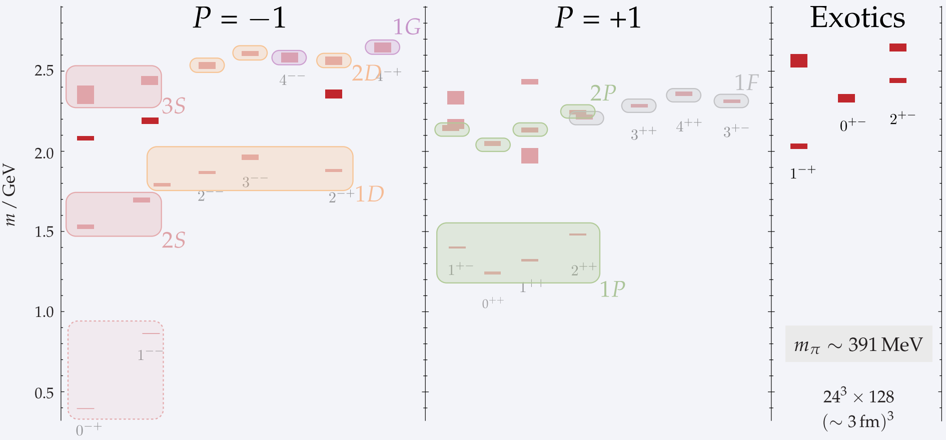

- Some states with ordinary J^{PC} do not fit into $q\bar{q}$ super-multiplets

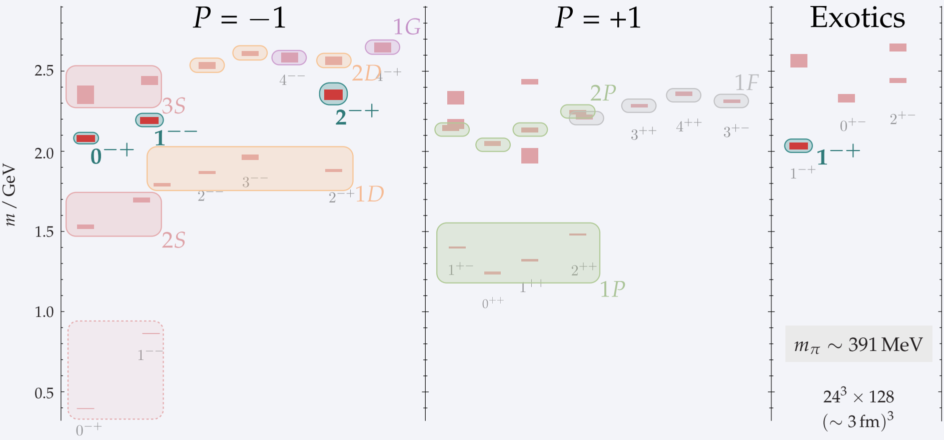

- Lightest hybrid meson super-multiplet with $J^{PC} = 1^{+-}$ gluonic excitation
- Resonance widths and decay modes still very difficult

Beyond the Constituent Quark Model

Finding states beyond the CQM is difficult

- Physical mesons = linear superpositions of *all* allowed basis states: $|q\bar{q}\rangle, |q\bar{q}g\rangle, |gg\rangle, |q^2\bar{q}^2\rangle, \ldots$
  - Amplitudes determined by QCD interactions
- Classification in quarkonia, hybrids, glueballs, tetraquarks, molecules, etc. assumes dominance of *one* basis state
  - In general "configuration mixing"
  - Disentanglement of contributions difficult

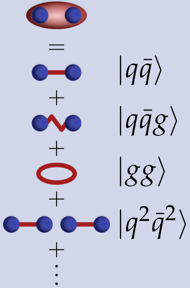

Special case: "**exotic**" **mesons**

- Have quantum numbers forbidden for $|q\bar{q}\rangle$
  - Discovery $\Longrightarrow$ unambiguous proof for meson states beyond CQM
- Especially attractive:
  "spin-exotic" states with $J^{PC} = \mathbf{0}^{--}, \mathbf{0}^{+-}, \mathbf{1}^{-+}, \mathbf{2}^{+-}, \mathbf{3}^{-+}, \ldots$

Beyond the Constituent Quark Model

Finding states beyond the CQM is difficult

- Physical mesons = linear superpositions of *all* allowed basis states: $|q\bar{q}\rangle, |q\bar{q}g\rangle, |gg\rangle, |q^2\bar{q}^2\rangle, \ldots$
  - Amplitudes determined by QCD interactions
- Classification in quarkonia, hybrids, glueballs, tetraquarks, molecules, etc. assumes dominance of *one* basis state
  - In general "configuration mixing"
  - Disentanglement of contributions difficult

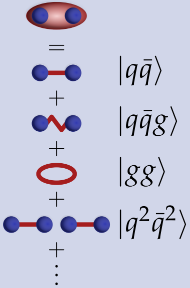

Special case: "**exotic**" **mesons**

- Have quantum numbers forbidden for $|q\bar{q}\rangle$
  - Discovery $\Longrightarrow$ unambiguous proof for meson states beyond CQM
- Especially attractive:
  "**spin-exotic**" states with $J^{PC} = \mathbf{0}^{--}, \mathbf{0}^{+-}, \mathbf{1}^{-+}, \mathbf{2}^{+-}, \mathbf{3}^{-+}, \ldots$

Beyond the Constituent Quark Model

Finding states beyond the CQM is difficult

- Physical mesons = linear superpositions of *all* allowed basis states: $|q\bar{q}\rangle, |q\bar{q}g\rangle, |gg\rangle, |q^2\bar{q}^2\rangle, \ldots$
  - Amplitudes determined by QCD interactions
- Classification in quarkonia, hybrids, glueballs, tetraquarks, molecules, etc. assumes dominance of *one* basis state
  - In general "configuration mixing"
  - Disentanglement of contributions difficult

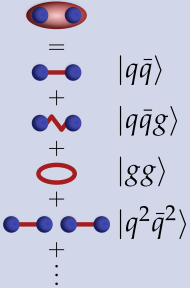

Special case: "**exotic**" mesons

- Have quantum numbers forbidden for $|q\bar{q}\rangle$
  - Discovery $\Longrightarrow$ unambiguous proof for meson states beyond CQM
- Especially attractive:
  "spin-exotic" states with $J^{PC} = \mathbf{0}^{--}, \mathbf{0}^{+-}, \mathbf{1}^{-+}, \mathbf{2}^{+-}, \mathbf{3}^{-+}, \ldots$

- "Light meson frontier"
  - Many missing and disputed excited states in mass region $m \approx 2\ \mathrm{GeV}/c^2$
- QCD predicts states beyond CQM
  - Much richer hadron spectrum: exotic or supernumerous states
    - Mixing with conventional $|q\bar{q}'\rangle$ states of same J^{PC}
    - Existence not yet proven

COMPASS

1. Explores light-quark meson spectrum in region $m \gtrsim 2\ \mathrm{GeV}/c^2$
2. Searches for states that do not fit into CQM scheme
3. Precision measurement of properties of known resonances

- "Light meson frontier"
  - Many missing and disputed excited states in mass region $m \approx 2\ \mathrm{GeV}/c^2$
- QCD predicts states beyond CQM
  - Much richer hadron spectrum: exotic or supernumerous states
    - Mixing with conventional $|q\bar{q}'\rangle$ states of same J^{PC}
    - Existence not yet proven

COMPASS

1. Explores light-quark meson spectrum in region $m \gtrsim 2\ \mathrm{GeV}/c^2$
2. Searches for states that do not fit into CQM scheme
3. Precision measurement of properties of known resonances

QCD and Constituent Quark Model
Summary

- "Light meson frontier"
  - Many missing and disputed excited states in mass region $m \approx 2\ \mathrm{GeV}/c^2$
- QCD predicts states beyond CQM
  - Much richer hadron spectrum: exotic or supernumerous states
    - Mixing with conventional $|q\bar{q}'\rangle$ states of same J^{PC}
    - Existence not yet proven

COMPASS

1. Explores light-quark meson spectrum in region $m \gtrsim 2\ \mathrm{GeV}/c^2$
2. Searches for states that do not fit into CQM scheme
3. Precision measurement of properties of known resonances

Outline

1. Introduction
   - QCD and the constituent quark model
   - Beyond the constituent quark model
2. How to measure meson spectra?
   - Meson production in diffractive dissociation
   - Partial-wave analysis method
3. Selected results
   - Partial-wave decomposition of the $(3\pi)^-$ final state
   - Resonance extraction in the $\pi^-\pi^+\pi^-$ system
4. Conclusions and outlook

Fixed-target experiment

- Two-stage spectrometer
- Large acceptance over wide kinematic range
- Electromagnetic and hadronic calorimeters
- Beam and final-state particle ID (CEDARs, RICH)

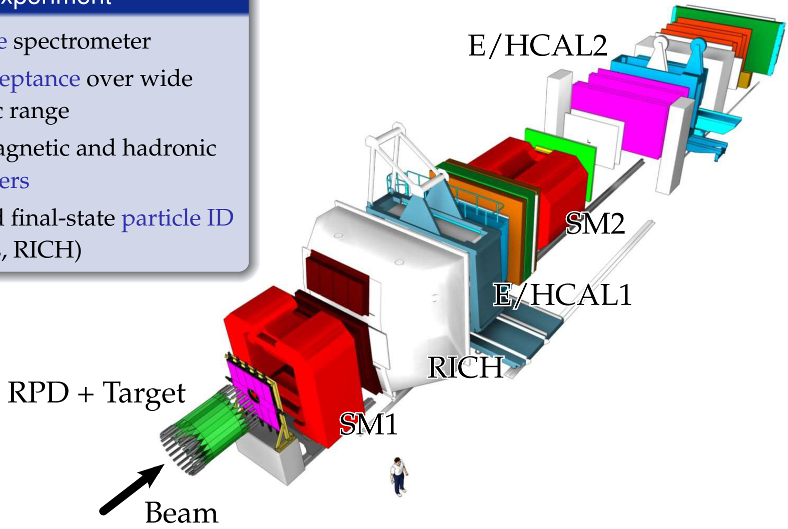

NIM A **577**, 455 (2007)

Fixed-target experiment

- Two-stage spectrometer
- Large acceptance over wide kinematic range
- Electromagnetic and hadronic calorimeters
- Beam and final-state particle ID (CEDARs, RICH)

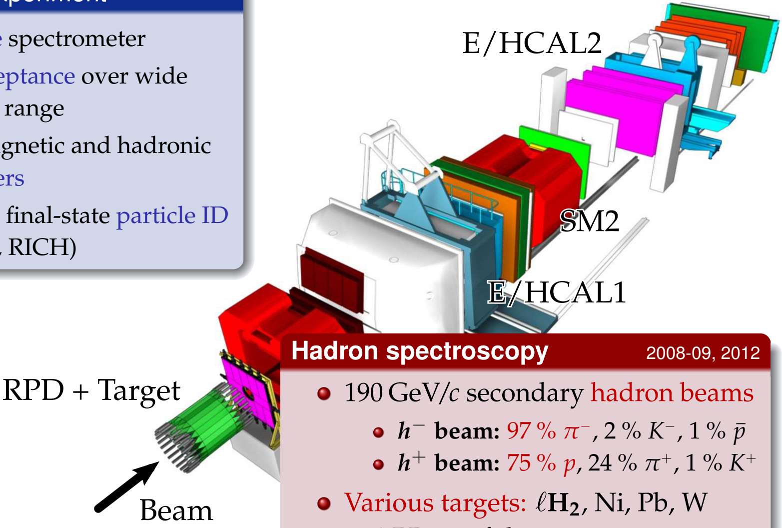

Hadron spectroscopy 2008-09, 2012

- 190 GeV/c secondary hadron beams
  - h^- **beam:** 97 % π^-, 2 % K^-, 1 % $\bar{p}$
  - h^+ **beam:** 75 % p, 24 % π^+, 1 % K^+
- Various targets: $\ell\mathbf{H_2}$, Ni, Pb, W
- $>$ 1 PByte of data per year

Meson Production in Diffractive Dissociation

Example: $\pi^- p \to \pi^- \pi^+ \pi^- p_{\text{recoil}}$

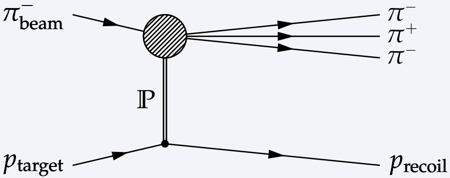

- Soft scattering of beam particle off target via strong interaction
  - Production of n forward-going hadrons (here $n = 3$)
  - Target particle stays intact
- All final-state particles are measured

Meson Production in Diffractive Dissociation

Example: $\pi^- p \to \pi^-\pi^+\pi^- p_{\text{recoil}}$

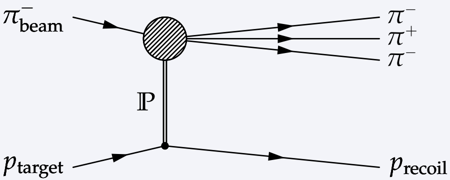

- Exclusive measurement
  - p_{recoil} measured by RPD
- Squared four-momentum transfer region $0.1 < t' < 1.0\ (\text{GeV}/c)^2$

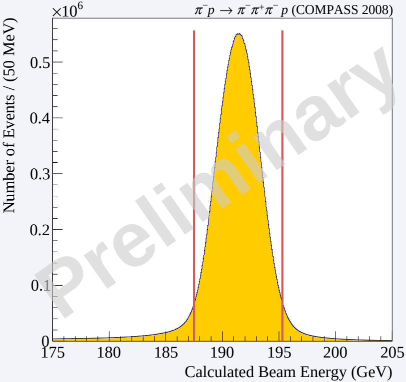

Meson Production in Diffractive Dissociation

Example: $\pi^- \, p \to \pi^- \pi^+ \pi^- \, p_{\text{recoil}}$

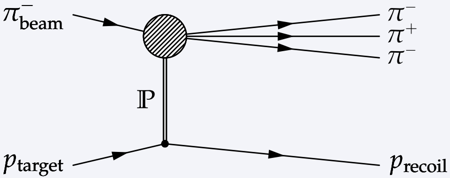

- Exclusive measurement
  - p_{recoil} measured by RPD
- Squared four-momentum transfer region $0.1 < t' < 1.0 \, (\text{GeV}/c)^2$

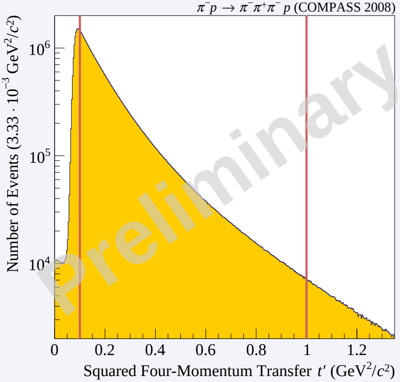

Meson Production in Diffractive Dissociation

Example: $\pi^- \, p \to \pi^- \pi^+ \pi^- \, p_{\text{recoil}}$

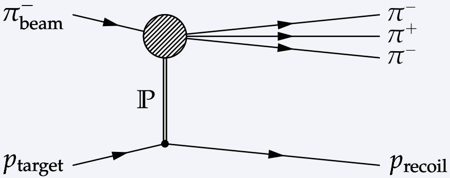

- Beam particle gets excited into intermediate resonance X
- X decays (dissociates) into n-body final state (here $n = 3$)
- Rich spectrum of intermediate states X

Meson Production in Diffractive Dissociation

Example: $\pi^- p \to \pi^- \pi^+ \pi^- p_{\text{recoil}}$

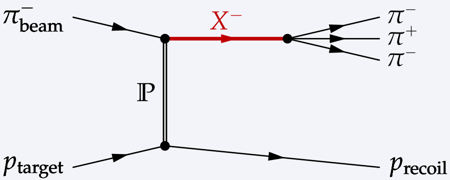

- **Beam** particle gets **excited into intermediate resonance** X
- X decays (dissociates) into n**-body final state** (here $n = 3$)
- Rich spectrum of intermediate states X

Meson Production in Diffractive Dissociation

Example: $\pi^- p \to \pi^-\pi^+\pi^- p_{\text{recoil}}$

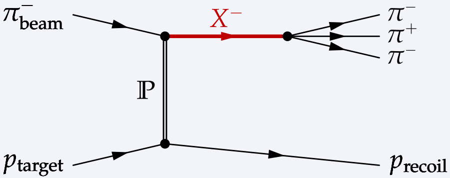

- Beam particle gets excited into intermediate resonance X
- X decays (dissociates) into n-body final state (here $n = 3$)
- Rich spectrum of intermediate states X

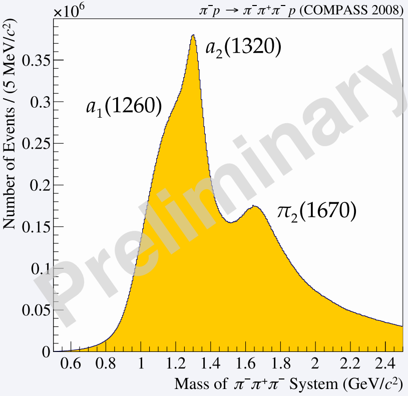

Meson Production in Diffractive Dissociation

Diffractive dissociation

- Many different intermediate states X decaying into same final state
- Intermediate states interfere

Goal: find all resonances

- Determine their mass, width, and quantum numbers

Method: **partial-wave analysis** (PWA)

- Uses full kinematic information in events
- Amplitude analysis: exploits interference of intermediate states
  - Additional phase information
  - Greatly helps to disentangle states

Meson Production in Diffractive Dissociation

Diffractive dissociation

- Many different intermediate states X decaying into same final state
- Intermediate states interfere

Goal: find all resonances

- Determine their mass, width, and quantum numbers

Method: **partial-wave analysis** (PWA)

- Uses full kinematic information in events
- Amplitude analysis: exploits interference of intermediate states
  - Additional phase information
  - Greatly helps to disentangle states

Meson Production in Diffractive Dissociation

Diffractive dissociation

- Many different intermediate states X decaying into same final state
- Intermediate states interfere

Goal: find all resonances

- Determine their mass, width, and quantum numbers

Method: **partial-wave analysis** (PWA)

- Uses full kinematic information in events
- Amplitude analysis: exploits interference of intermediate states
  - Additional phase information
  - Greatly helps to disentangle states

The Power of Phase Information

. . . or: From Bump Hunting to Amplitude Analysis

Analogy: phase-contrast imaging

M. Bech *et al.*, Sci. Rep. **3** (2013) 3209

X-ray attenuation image

X-ray phase-contrast image

"Bump hunting"

"Amplitude Analysis"

Analogy: phase-contrast imaging

M. Bech *et al.*, Sci. Rep. **3** (2013) 3209

X-ray attenuation image

"Bump hunting"

X-ray phase-contrast image

"Amplitude Analysis"

The Power of Phase Information

... or: From Bump Hunting to Amplitude Analysis

Analogy: phase-contrast imaging — M. Bech *et al.*, Sci. Rep. **3** (2013) 3209

X-ray attenuation image

“Bump hunting”

X-ray phase-contrast image

“Amplitude Analysis”

The Power of Phase Information

. . . or: From Bump Hunting to Amplitude Analysis

Example: amplitude of a single narrow relativistic Breit-Wigner resonance

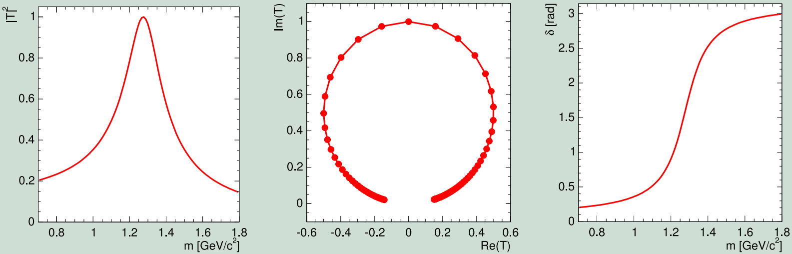

Peters, arxiv:hep-ph/0412069

- Resonance lies on unitarity circle
  - Elastic case
- **"Phase motion":** δ rises from 0 to π and is $\pi/2$ at peak position
  - Analogous to mechanical oscillator

Partial-Wave Analysis: $\pi^-\pi^+\pi^-$ Final State

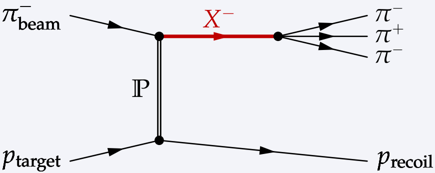

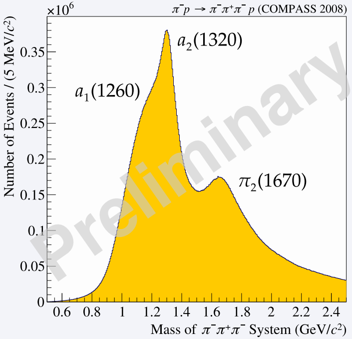

X^- does *not* decay directly into $\pi^-\pi^+\pi^-$

Partial-Wave Analysis: $\pi^-\pi^+\pi^-$ Final State

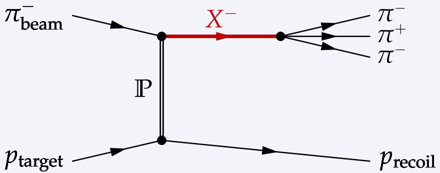

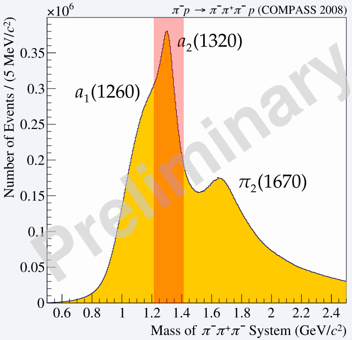

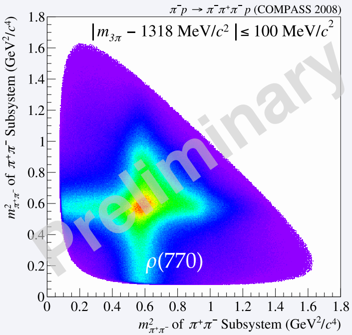

X^- does *not* decay directly into $\pi^-\pi^+\pi^-$

Partial-Wave Analysis: $\pi^-\pi^+\pi^-$ Final State

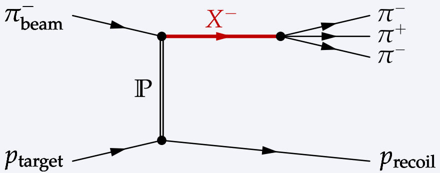

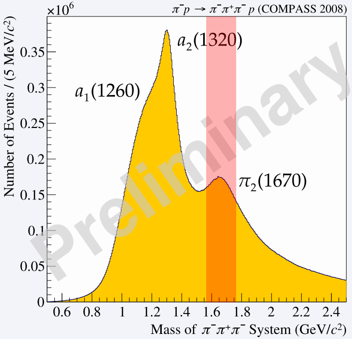

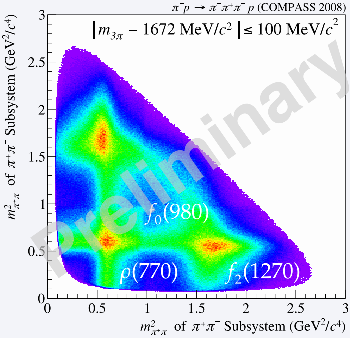

X^- does *not* decay directly into $\pi^-\pi^+\pi^-$

Partial-Wave Analysis: $\pi^-\pi^+\pi^-$ Final State

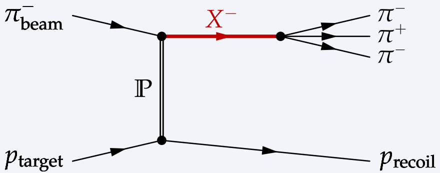

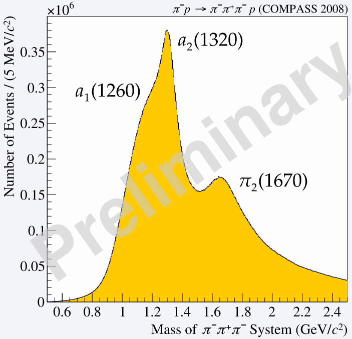

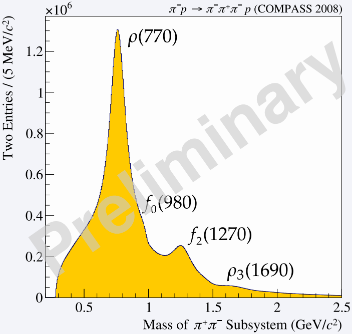

X^- does *not* decay directly into $\pi^-\pi^+\pi^-$

Partial-Wave Analysis: $\pi^-\pi^+\pi^-$ Final State

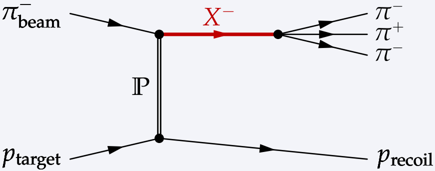

Isobar model

- X^- decays via intermediate $\pi^+\pi^-$ resonance = *"isobar"*
  - $[\pi\pi]_{\text{S-wave}}$ $J^{PC} = 0^{++}$
  - $\rho(770)$ 1^{--}
  - $f_0(980)$ 0^{++}
  - $f_2(1270)$ 2^{++}
  - $f_0(1500)$ 0^{++}
  - $\rho_3(1690)$ 3^{--}

Partial-Wave Analysis: $\pi^-\pi^+\pi^-$ Final State

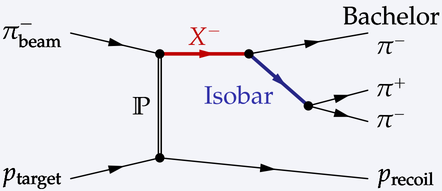

Isobar model

- X^- decays via intermediate $\pi^+\pi^-$ resonance = *"isobar"*
  - $[\pi\pi]_{\text{S-wave}}$ $J^{PC} = 0^{++}$
  - $\rho(770)$ 1^{--}
  - $f_0(980)$ 0^{++}
  - $f_2(1270)$ 2^{++}
  - $f_0(1500)$ 0^{++}
  - $\rho_3(1690)$ 3^{--}

Partial-Wave Analysis: $\pi^-\pi^+\pi^-$ Final State

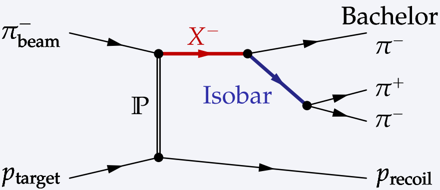

Isobar model

- X^- decays via intermediate $\pi^+\pi^-$ resonance = *"isobar"*
  - $[\pi\pi]_{\text{S-wave}}$ $J^{PC} = 0^{++}$
  - $\rho(770)$ 1^{--}
  - $f_0(980)$ 0^{++}
  - $f_2(1270)$ 2^{++}
  - $f_0(1500)$ 0^{++}
  - $\rho_3(1690)$ 3^{--}

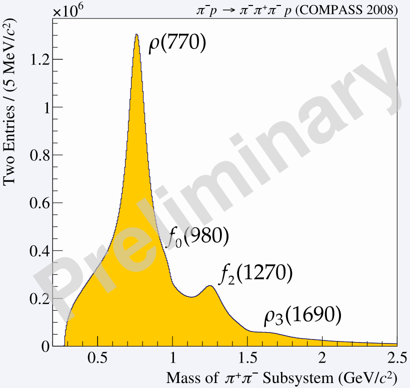

Partial-Wave Analysis: $\pi^-\pi^+\pi^-$ Final State

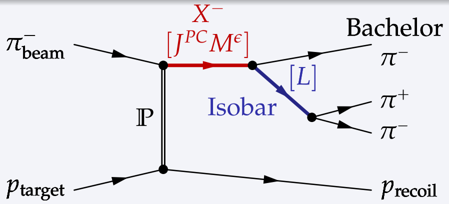

Isobar model

- Isobar has spin S and relative orbital angular momentum L w.r.t. bachelor π^-
  - L and S couple to spin J of X^-
- **"Wave"** $=$ unique combination of isobar and quantum numbers
- *Notation:* $J^{PC}\,M^\epsilon$ isobar πL
- 3-body kinematics fixed by m_X plus 5 phase space variables τ
- **Decay amplitude** $A_{\text{wave}}(m_X, \tau)$
  - Describes τ distribution for given wave $\Longrightarrow$ **Calculable!**

Partial-Wave Analysis: $\pi^-\pi^+\pi^-$ Final State

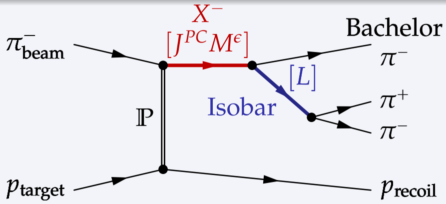

Isobar model

- Isobar has spin S and relative orbital angular momentum L w.r.t. bachelor π^-
  - L and S couple to spin J of X^-
- **"Wave"** = unique combination of isobar and quantum numbers
- *Notation:* $J^{PC}\,M^{\epsilon}$ isobar πL
- 3-body kinematics fixed by m_X plus 5 phase space variables τ
- **Decay amplitude** $A_{\text{wave}}(m_X, \tau)$
  - Describes τ distribution for given wave $\Longrightarrow$ **Calculable!**

Partial-Wave Analysis: $\pi^-\pi^+\pi^-$ Final State

Example: angular distribution for $2^{-+}1^+ f_2(1270)\pi D$ wave

Resonance decay

$X^-(2^{-+}) \to f_2(1270)\pi^-$

Isobar decay

$f_2(1270) \to \pi^+\pi^-$

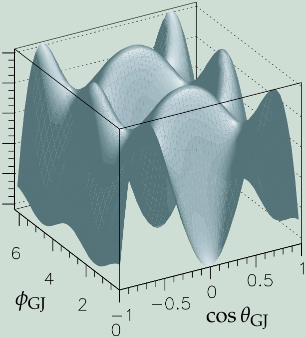

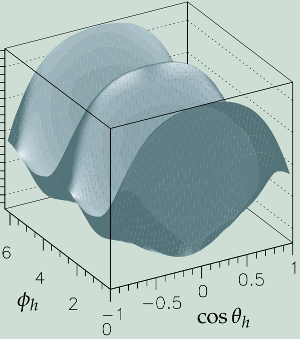

Dzierba *et al.*, PR **D73** (2006) 072001

- 2D projections of a genuine 5D distribution ($m_X = \text{const.}$)
  - f_2 and π^- in relative D-wave
  - $f_2(1270)$: $J^P = 2^+ \implies \pi^+\pi^-$ in relative D-wave

Partial-Wave Analysis: $\pi^-\pi^+\pi^-$ Final State

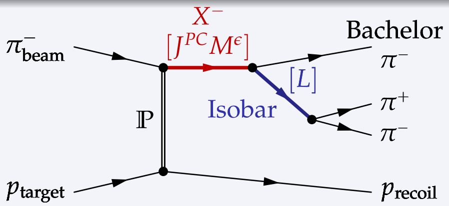

Isobar model

- *Ansatz:* Production of X is independent of its decay
  - Production described by amplitudes $T_{\text{wave}}(m_X)$
    - Strength and relative phase of partial wave
  - Total amplitude of a wave is $T_{\text{wave}}(m_X)\,A_{\text{wave}}(\tau; m_X)$
- Many waves contribute
  - Same final state $\Longrightarrow$ amplitudes have to be summed coherently
- Intensity: $\mathcal{I}(\tau; m_X) = \left|\sum_{\text{waves}} T_{\text{wave}}(m_X)\,A_{\text{wave}}(\tau; m_X)\right|^2$
  - Model for τ distribution with unknown parameters $T_{\text{wave}}(m_X)$

Partial-Wave Analysis: $\pi^-\pi^+\pi^-$ Final State

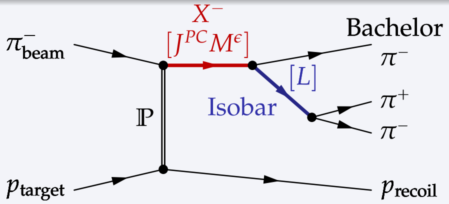

Isobar model

- *Ansatz:* Production of X is independent of its decay
  - Production described by amplitudes $T_{\text{wave}}(m_X)$
    - Strength and relative phase of partial wave
  - Total amplitude of a wave is $T_{\text{wave}}(m_X)\, A_{\text{wave}}(\tau; m_X)$
- Many waves contribute
  - Same final state $\Longrightarrow$ amplitudes have to be summed coherently
- Intensity: $\mathcal{I}(\tau; m_X) = \left| \sum_{\text{waves}} T_{\text{wave}}(m_X)\, A_{\text{wave}}(\tau; m_X) \right|^2$
  - Model for τ distribution with unknown parameters $T_{\text{wave}}(m_X)$

Partial-Wave Analysis: $\pi^-\pi^+\pi^-$ Final State

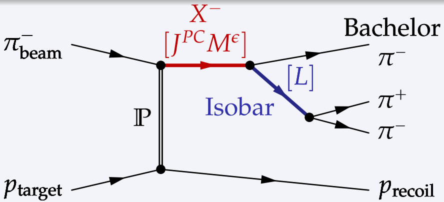

Isobar model: spin-parity decomposition

- Intensity: $\mathcal{I}(\tau; m_X) = \left|\sum_{\text{waves}} T_{\text{wave}}(m_X)\, A_{\text{wave}}(\tau; m_X)\right|^2$
- Determination of $T_{\text{wave}}(m_X)$
  1. Bin data in m_X
     - Neglect m_X dependence within mass bin
     - No assumptions about 3π resonances
  2. Maximum likelihood fit of 5-dimensional τ distribution in each m_X
     - Takes into account detector acceptance and efficiency
     - Decomposition into (nearly) orthonormal function system $\{A_{\text{wave}}(\tau)\}$

Partial-Wave Analysis: $\pi^-\pi^+\pi^-$ Final State

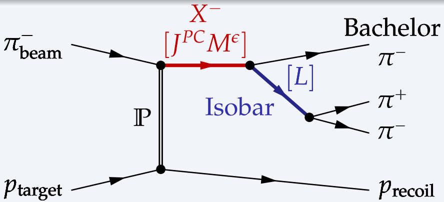

Isobar model: spin-parity decomposition

- Intensity: $\mathcal{I}(\tau; m_X) = \left|\sum_{\text{waves}} T_{\text{wave}}(m_X)\, A_{\text{wave}}(\tau; m_X)\right|^2$
- **Determination of $T_{\text{wave}}(m_X)$**
  1. Bin data in m_X
     - Neglect m_X dependence within mass bin
     - No assumptions about 3π resonances
  2. Maximum likelihood fit of 5-dimensional τ distribution in each m_X
     - Takes into account detector acceptance and efficiency
     - Decomposition into (nearly) orthonormal function system $\{A_{\text{wave}}(\tau)\}$

Partial-Wave Analysis: $\pi^-\pi^+\pi^-$ Final State

Truncation of the Partial-Wave Series

- Intensity: $\mathcal{I}(\tau; m_X) = \left|\sum_{\text{waves}}^{\infty} T_{\text{wave}}(m_X)\, A_{\text{wave}}(\tau; m_X)\right|^2$
- In principle infinitely many partial waves
  - All allowed isobars and orbital angular momentum values
- Limited amount of data $\Longrightarrow$ truncate series
  - Dominant isobars determined from kinematic distributions of isobar subsystems (e.g. $m_{\pi^+\pi^-}$ distribution)
  - Selection of waves based on physics and experience
    - Iterative optimization process

Wave set used for analysis of 3π data

- 87 waves + incoherent isotropic background ("flat") wave
  - By far the largest wave set ever used for this channel
  - Spin J up to 6
  - Orbital angular momentum L up to 6
  - Isobars: $(\pi\pi)_S$, $f_0(980)$, $\rho(770)$, $f_2(1270)$, $f_0(1500)$ and $\rho_3(1690)$

Partial-Wave Analysis: $\pi^-\pi^+\pi^-$ Final State

Truncation of the Partial-Wave Series

- Intensity: $\mathcal{I}(\tau; m_X) = \left|\sum_{\text{waves}}^{\infty} T_{\text{wave}}(m_X)\, A_{\text{wave}}(\tau; m_X)\right|^2$
- In principle infinitely many partial waves
  - All allowed isobars and orbital angular momentum values
- Limited amount of data $\Longrightarrow$ truncate series
  - Dominant isobars determined from kinematic distributions of isobar subsystems (e.g. $m_{\pi^+\pi^-}$ distribution)
  - Selection of waves based on physics and experience
    - Iterative optimization process

Wave set used for analysis of 3π data

- 87 waves + incoherent isotropic background ("flat") wave
  - By far the largest wave set ever used for this channel
  - Spin J up to 6
  - Orbital angular momentum L up to 6
  - Isobars: $(\pi\pi)_S$, $f_0(980)$, $\rho(770)$, $f_2(1270)$, $f_0(1500)$ and $\rho_3(1690)$

Outline

1. Introduction
   - QCD and the constituent quark model
   - Beyond the constituent quark model
2. How to measure meson spectra?
   - Meson production in diffractive dissociation
   - Partial-wave analysis method
3. Selected results
   - Partial-wave decomposition of the $(3\pi)^-$ final state
   - Resonance extraction in the $\pi^-\pi^+\pi^-$ system
4. Conclusions and outlook

PWA of $\pi^- p \to (3\pi)^- p_{\text{recoil}}$: Data Sets

$\approx 50 \cdot 10^6$ exclusive $\pi^-\pi^+\pi^-$ events

- World's largest $\pi^-\pi^+\pi^-$ data set by far
- Kinematic range $0.1 < t' < 1.0\,(\text{GeV}/c)^2$
- Challenging analysis
  - Requires large computing resources
  - Needs precise understanding of apparatus
  - Systematics larger than statistical uncertainties

Crosscheck systematics using $\pi^-\pi^0\pi^0$ events

- 3.5 M exclusive events
- Very different acceptance
- Isobars separated by isospin
  - $I = 1$ isobars: $\pi^-\pi^0$
  - $I = 0$ isobars: $\pi^0\pi^0$

PWA of $\pi^- p \to (3\pi)^- p_{\text{recoil}}$: Data Sets

$\approx 50 \cdot 10^6$ exclusive $\pi^-\pi^+\pi^-$ events

- World's largest $\pi^-\pi^+\pi^-$ data set by far
- Kinematic range $0.1 < t' < 1.0\,(\text{GeV}/c)^2$
- Challenging analysis
  - Requires large computing resources
  - Needs precise understanding of apparatus
  - Systematics larger than statistical uncertainties

Crosscheck systematics using $\pi^-\pi^0\pi^0$ events

- 3.5 M exclusive events
- Very different acceptance
- Isobars separated by isospin
  - $I = 1$ isobars: $\pi^-\pi^0$
  - $I = 0$ isobars: $\pi^0\pi^0$

PWA of $\pi^- p \to (3\pi)^- p_{\text{recoil}}$: A Complication

- 3π invariant mass spectrum depends on t'
  - Partial waves have different t' dependencies
- t' spectrum depends on 3π invariant mass
- Modeling of t' dependence difficult
- Avoid model bias by binning data in t' and $m_{3\pi}$
  - 11 t' bins for $\pi^-\pi^+\pi^-$ and 8 t' bins for $\pi^-\pi^0\pi^0$

$0.10 < t' < 0.12\ (\text{GeV}/c)^2$

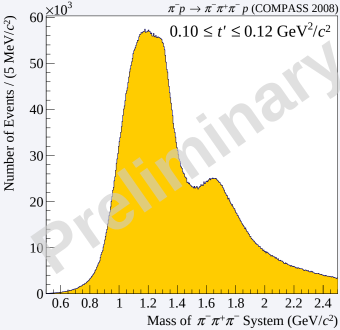

$0.44 < t' < 1.00\ (\text{GeV}/c)^2$

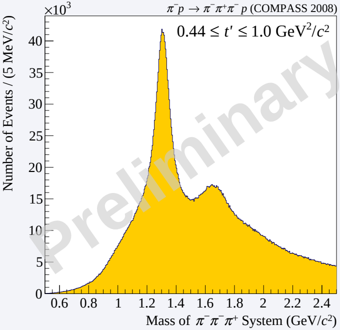

PWA of $\pi^- p \to (3\pi)^- p_{\text{recoil}}$: A Complication

- 3π invariant mass spectrum depends on t'
  - Partial waves have different t' dependencies
- t' spectrum depends on 3π invariant mass
- Modeling of t' dependence difficult
- Avoid model bias by binning data in t' and $m_{3\pi}$
  - 11 t' bins for $\pi^-\pi^+\pi^-$ and 8 t' bins for $\pi^-\pi^0\pi^0$

$800 < m_{3\pi} < 850$ MeV/c^2

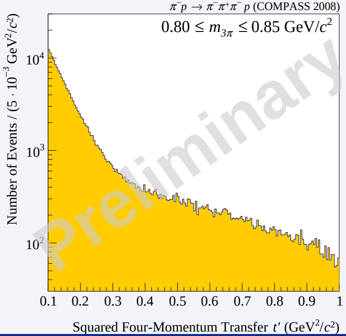

$1600 < m_{3\pi} < 1650$ MeV/c^2

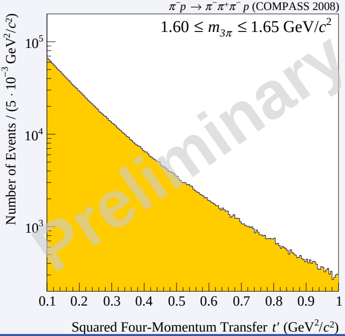

PWA of $\pi^- p \to (3\pi)^- p_{\text{recoil}}$: A Complication

- 3π invariant mass spectrum depends on t'
  - Partial waves have different t' dependencies
- t' spectrum depends on 3π invariant mass
- Modeling of t' dependence difficult
- Avoid model bias by binning data in t' and $m_{3\pi}$
  - 11 t' bins for $\pi^-\pi^+\pi^-$ and 8 t' bins for $\pi^-\pi^0\pi^0$

$800 < m_{3\pi} < 850\ \text{MeV}/c^2$

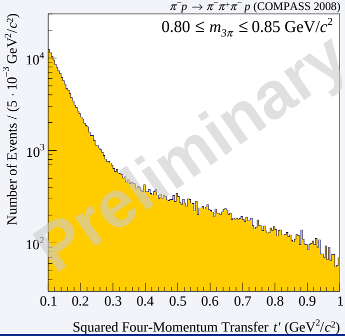

$1600 < m_{3\pi} < 1650\ \text{MeV}/c^2$

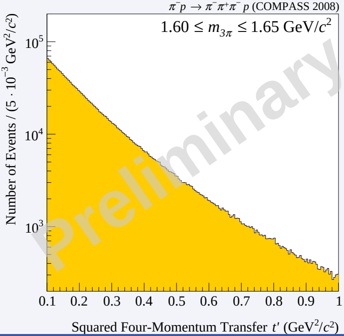

PWA of $\pi^- p \to (3\pi)^- p_{\text{recoil}}$: Major Waves

- $\pi^-\pi^+\pi^-$ invariant mass spectrum
- $1^{++}0^+ \rho\pi S$: $a_1(1260)$
- $2^{++}1^+ \rho\pi D$: $a_2(1320)$
- $2^{-+}0^+ f_2\pi S$: $\pi_2(1670)$

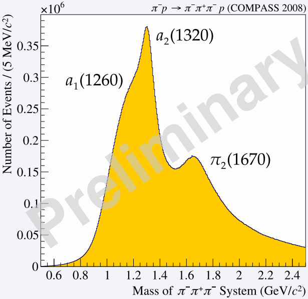

$\pi^-\pi^0\pi^0$

$\pi^-\pi^+\pi^-$ scaled for each plot

PWA of $\pi^- p \to (3\pi)^- p_{\text{recoil}}$: Major Waves

- $\pi^-\pi^+\pi^-$ invariant mass spectrum
- $1^{++}0^+ \rho\pi S$: $a_1(1260)$
- $2^{++}1^+ \rho\pi D$: $a_2(1320)$
- $2^{-+}0^+ f_2\pi S$: $\pi_2(1670)$

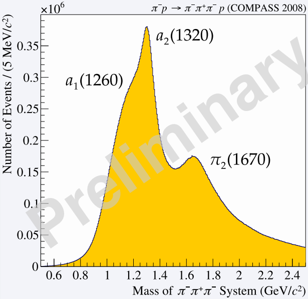

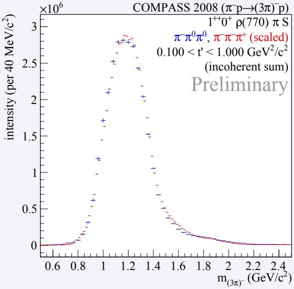

$\pi^-\pi^0\pi^0$

$\pi^-\pi^+\pi^-$ scaled for each plot

PWA of $\pi^- p \to (3\pi)^- p_{\text{recoil}}$: Major Waves

- $\pi^-\pi^+\pi^-$ invariant mass spectrum
- $1^{++}0^+ \rho\pi S$: $a_1(1260)$
- $2^{++}1^+ \rho\pi D$: $a_2(1320)$
- $2^{-+}0^+ f_2\pi S$: $\pi_2(1670)$

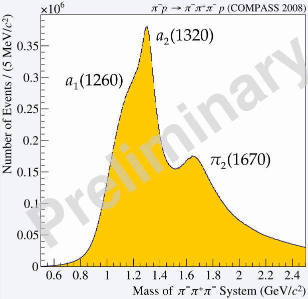

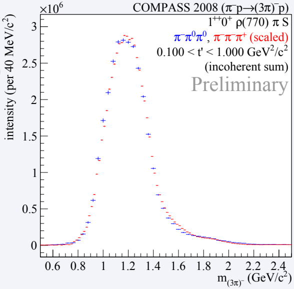

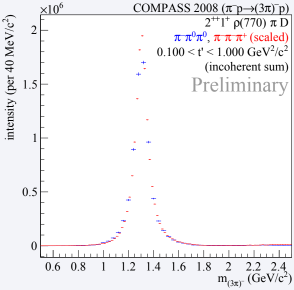

$\pi^-\pi^0\pi^0$

$\pi^-\pi^+\pi^-$ scaled for each plot

PWA of $\pi^- p \to (3\pi)^- p_{\text{recoil}}$: Major Waves

- $\pi^-\pi^+\pi^-$ invariant mass spectrum
- $1^{++}0^+ \rho\pi S$: $a_1(1260)$
- $2^{++}1^+ \rho\pi D$: $a_2(1320)$
- $2^{-+}0^+ f_2\pi S$: $\pi_2(1670)$

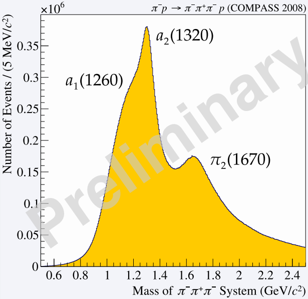

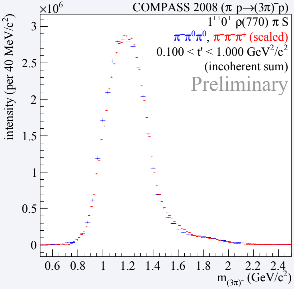

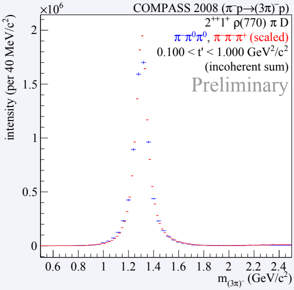

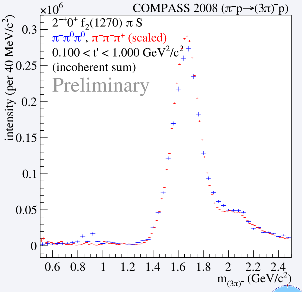

$\pi^-\pi^0\pi^0$

$\pi^-\pi^+\pi^-$ scaled for each plot

PWA of $\pi^- p \to (3\pi)^- p_{\text{recoil}}$: Low t' vs. High t'

$2^{++}1^+ \rho\pi D$

- Peak does not change with t'

$1^{++}0^+ \rho\pi S$

- Peak *moves* with t'
- Strong non-resonant contribution

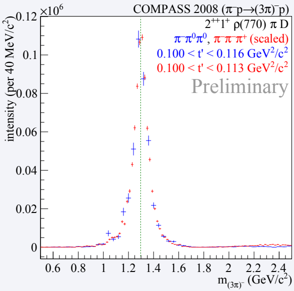

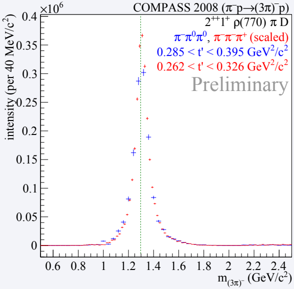

$\pi^-\pi^0\pi^0$

$\pi^-\pi^+\pi^-$ scaled for each plot

PWA of $\pi^- p \to (3\pi)^- p_{\text{recoil}}$: Low t' vs. High t'

$2^{++}1^+ \rho\pi D$

- Peak does not change with t'

$1^{++}0^+ \rho\pi S$

- Peak *moves* with t'
- Strong non-resonant contribution

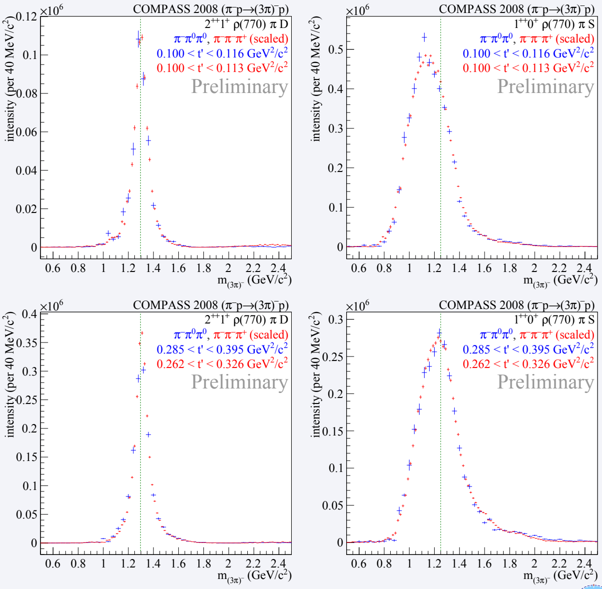

$\pi^-\pi^0\pi^0$

$\pi^-\pi^+\pi^-$ scaled for each plot

PWA of $\pi^- p \to (3\pi)^- p_{\text{recoil}}$: Selected Small Waves

$4^{++}\,1^+\,\rho\pi G$

- $a_4(2040)$

$0^{-+}\,0^+\,f_0(980)\pi S$

- $\pi(1800)$

$1^{++}\,0^+\,f_0(980)\pi P$

- **New signal around 1.4 GeV/c^2**
- Very small intensity

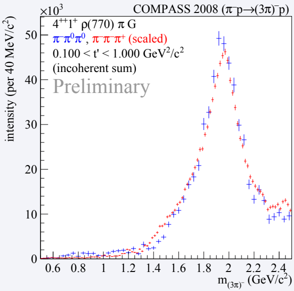

$\pi^-\pi^0\pi^0$

$\pi^-\pi^+\pi^-$ scaled for each plot

PWA of $\pi^- p \to (3\pi)^- p_{\text{recoil}}$: Selected Small Waves

$4^{++}\,1^+\,\rho\pi G$

- $a_4(2040)$

$0^{-+}\,0^+\,f_0(980)\pi S$

- $\pi(1800)$

$1^{++}\,0^+\,f_0(980)\pi P$

- **New signal around 1.4 GeV/c^2**
- Very small intensity

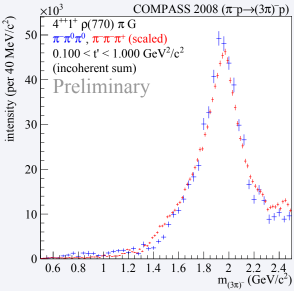

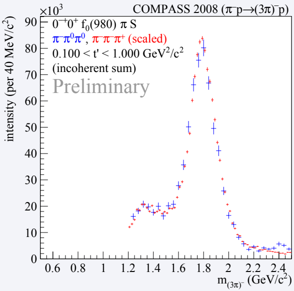

$\pi^-\pi^0\pi^0$

$\pi^-\pi^+\pi^-$ scaled for each plot

PWA of $\pi^- p \to (3\pi)^- p_{\text{recoil}}$: Selected Small Waves

$4^{++} 1^+ \rho\pi G$

- $a_4(2040)$

$0^{-+} 0^+ f_0(980)\pi S$

- $\pi(1800)$

$1^{++} 0^+ f_0(980)\pi P$

- **New signal around 1.4 GeV/c^2**
- Very small intensity

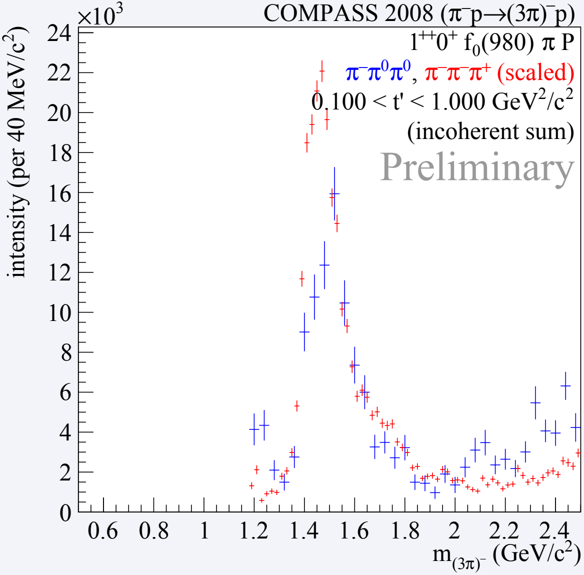

$\pi^-\pi^0\pi^0$

$\pi^-\pi^+\pi^-$ scaled for each plot

PWA of $\pi^- p \to (3\pi)^- p_{\text{recoil}}$: 1^{-+} Spin-Exotic Wave

$1^{-+}\, 1^+\, \rho\pi P$

- Broad intensity bump
- Similar in both channels
- Strong modulation with t'
- Slow phase motion in all t' bins

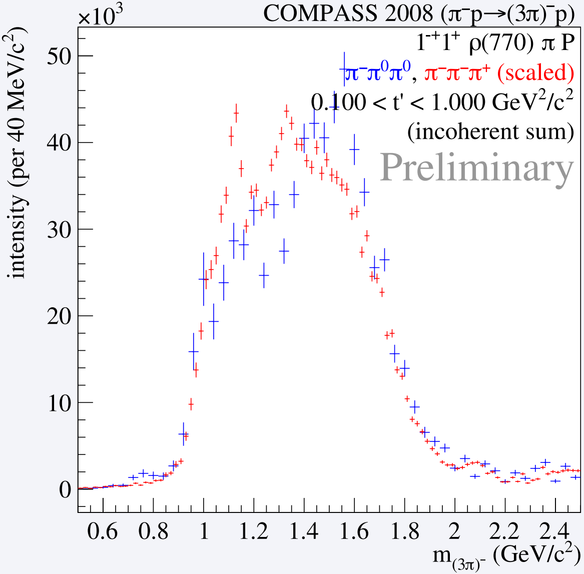

$\pi^-\pi^0\pi^0$

$\pi^-\pi^+\pi^-$ scaled for each plot

PWA of $\pi^- p \to (3\pi)^- p_{\text{recoil}}$: 1^{-+} Spin-Exotic Wave

$1^{-+}1^{+}\rho\pi P$

- Broad intensity bump
- Similar in both channels
- Strong modulation with t'
- Slow phase motion in all t' bins

$\pi^-\pi^+\pi^-$ data

Deck MC scaled to t'-integrated intensity

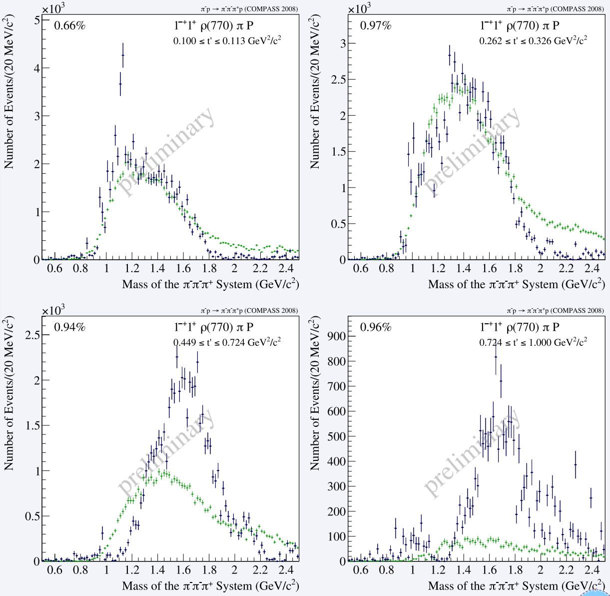

PWA of $\pi^- p \to (3\pi)^- p_{\text{recoil}}$: 1^{-+} Spin-Exotic Wave

$1^{-+}1^{+}\rho\pi P$

- Broad intensity bump
- Similar in both channels
- Strong modulation with t'
- Slow phase motion in all t' bins

$\pi^-\pi^+\pi^-$ data

Deck MC scaled to t'-integrated intensity

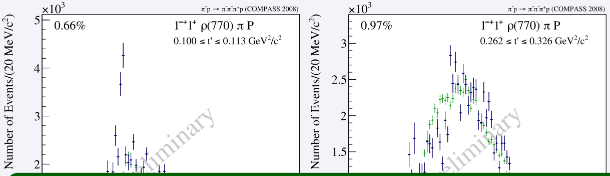

Monte Carlo simulation of Deck effect

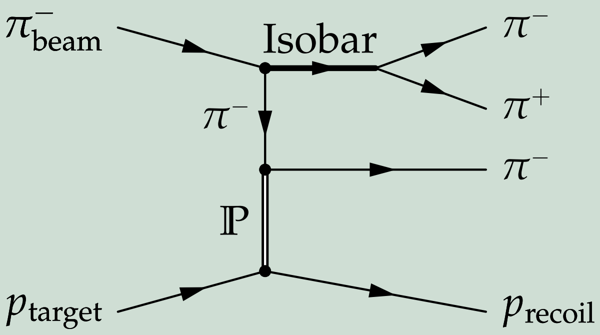

PWA of $\pi^- p \to (3\pi)^- p_{\text{recoil}}$: 1^{-+} Spin-Exotic Wave

$1^{-+}1^{+}\rho\pi P$

- Broad intensity bump
- Similar in both channels
- Strong modulation with t'
- Slow phase motion in all t' bins

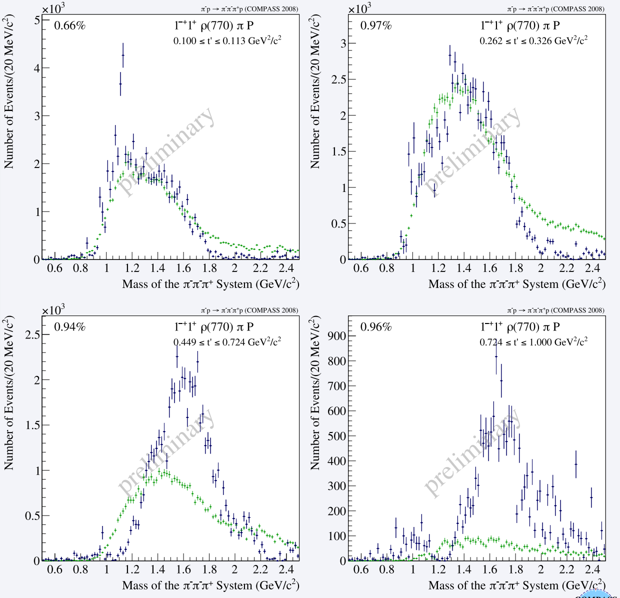

$\pi^-\pi^+\pi^-$ data

Deck MC scaled to t'-integrated intensity

PWA of $\pi^- p \to (3\pi)^- p_{\text{recoil}}$: 1^{-+} Spin-Exotic Wave

$1^{-+}1^+ \rho\pi P$

- Broad intensity bump
- Similar in both channels
- Strong modulation with t'
- Slow phase motion in all t' bins

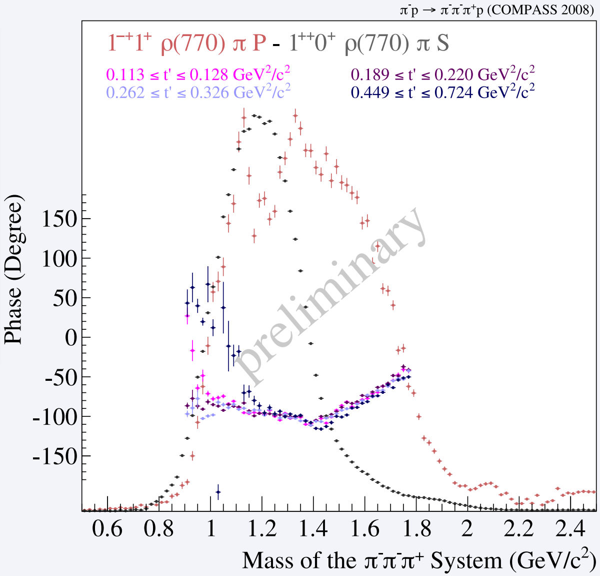

PWA of $\pi^- p \to \pi^-\pi^+\pi^- p_{\text{recoil}}$: Fit of Mass Dependence

Extraction of resonance parameters

- Model mass dependence of subset of 6 partial waves
  1. $1^{++}0^+ \rho\pi S$ — $a_1(1260) + a_1'$
  2. $2^{++}1^+ \rho\pi D$ — $a_2(1320) + a_2'$
  3. $2^{-+}0^+ f_2\pi S$ — $\pi_2(1670) + \pi_2(1880)$
  4. $4^{++}1^+ \rho\pi G$ — $a_4(2040)$
  5. $0^{-+}0^+ f_0(980)\pi S$ — $\pi(1800)$
  6. $1^{++}0^+ f_0(980)\pi P$ — $a_1(1420)$
  - Resonances: relativistic Breit-Wigner amplitudes
  - Coherent non-resonant term in each wave: phenomenological parametrization
  - Parameters estimation by χ^2 fit

Novel method: Combined fit of all t' bins

- Same resonance parameters in each t' bin
- Improves separation of resonant and non-resonant contributions

PWA of $\pi^- p \to \pi^-\pi^+\pi^- p_{\text{recoil}}$: Fit of Mass Dependence

Extraction of resonance parameters

- Model mass dependence of subset of 6 partial waves

1. $1^{++}0^+ \rho\pi S$ — $a_1(1260)$ $+ a_1{}'$
2. $2^{++}1^+ \rho\pi D$ — $a_2(1320)$ $+ a_2{}'$
3. $2^{-+}0^+ f_2\pi S$ — $\pi_2(1670)$ $+ \pi_2(1880)$
4. $4^{++}1^+ \rho\pi G$ — $a_4(2040)$
5. $0^{-+}0^+ f_0(980)\pi S$ — $\pi(1800)$
6. $1^{++}0^+ f_0(980)\pi P$ — $a_1(1420)$

  - Resonances: relativistic Breit-Wigner amplitudes
  - Coherent non-resonant term in each wave: phenomenological parametrization
  - Parameters estimation by χ^2 fit

Novel method: Combined fit of all t' bins

- Same resonance parameters in each t' bin
- Improves separation of resonant and non-resonant contributions

PWA of $\pi^- p \to \pi^-\pi^+\pi^- p_{\text{recoil}}$: Fit of Mass Dependence

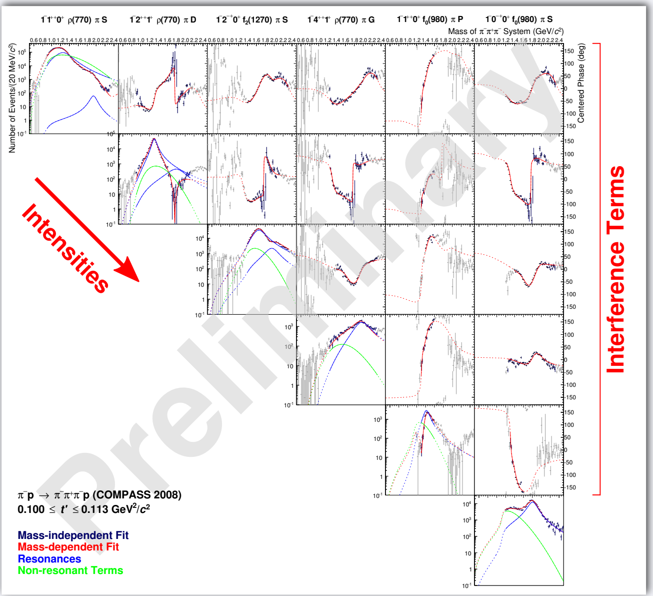

PWA of $\pi^- p \to \pi^- \pi^+ \pi^- p_{\text{recoil}}$: Fit of Mass Dependence

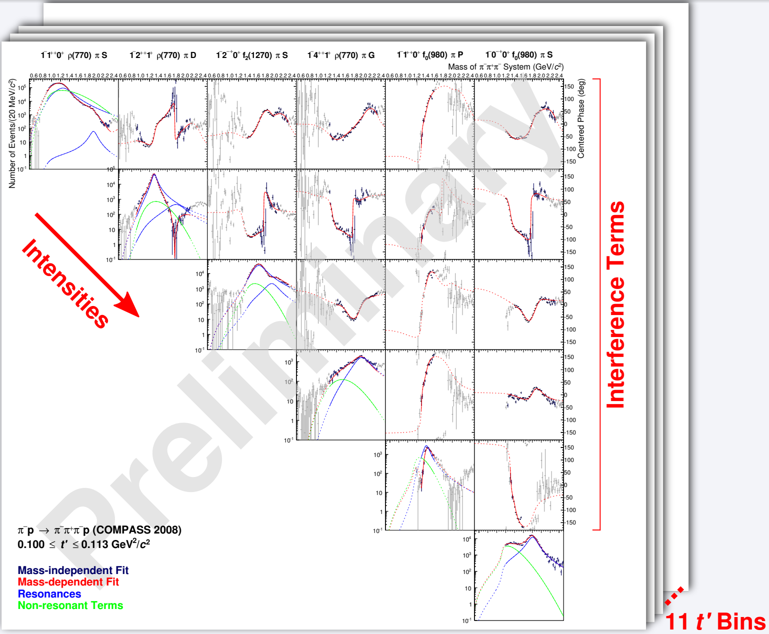

PWA of $\pi^- p \to \pi^-\pi^+\pi^- p_{\text{recoil}}$: Fit of Mass Dependence

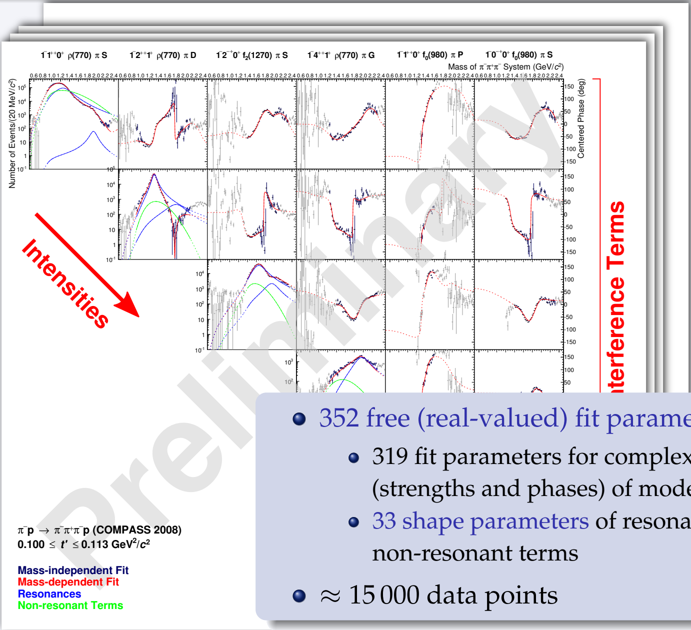

- 352 free (real-valued) fit parameters
  - 319 fit parameters for complex amplitudes (strengths and phases) of model components
  - 33 shape parameters of resonances and non-resonant terms
- $\approx 15\,000$ data points

PWA of $\pi^- p \to \pi^-\pi^+\pi^- p_{\text{recoil}}$: Fit of Mass Dependence

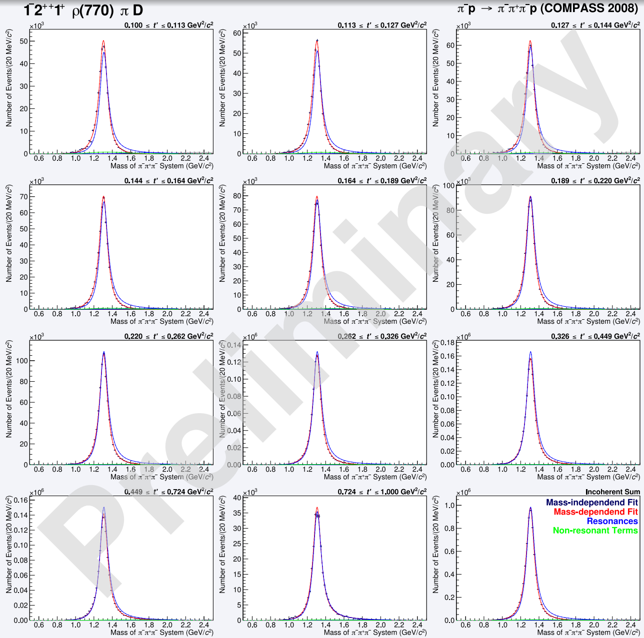

$2^{++}\,1^{+}\,\rho\pi D$

$a_2(1320)$ parameters

- $m = 1312\text{-}1315\ \text{MeV}/c^2$
- $\Gamma = 108\text{-}115\ \text{MeV}/c^2$

Cf. PDG 2012

- $m = 1318.3^{+0.5}_{-0.6}\ \text{MeV}/c^2$
- $\Gamma = 107 \pm 5\ \text{MeV}/c^2$

a_2' parameters

- $m = 1740\text{–}1890\ \text{MeV}/c^2$
- $\Gamma = 300\text{–}555\ \text{MeV}/c^2$

cf. PDG 2012 “omitted from summary”: $a_2(1700)$

- $m = 1732 \pm 16\ \text{MeV}/c^2$
- $\Gamma = 194 \pm 40\ \text{MeV}/c^2$

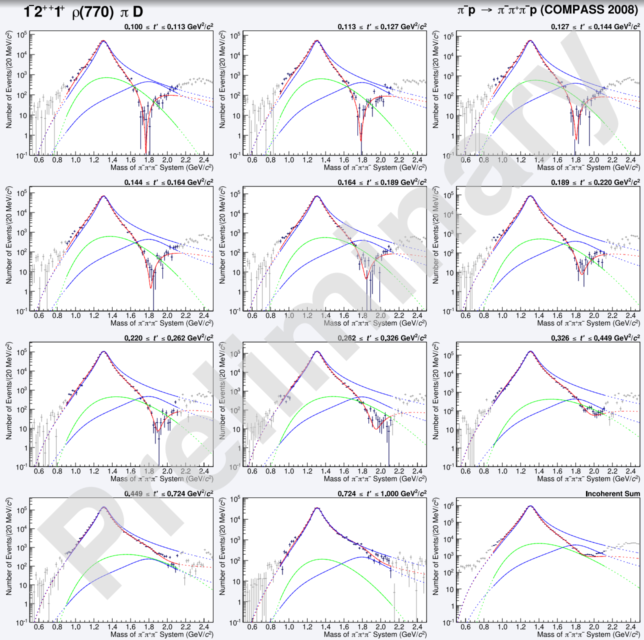

$2^{++}\,1^{+}\,\rho\pi D$

$a_2(1320)$ parameters

- $m = 1312\text{-}1315\ \text{MeV}/c^2$
- $\Gamma = 108\text{-}115\ \text{MeV}/c^2$

Cf. PDG 2012

- $m = 1318.3^{+0.5}_{-0.6}\ \text{MeV}/c^2$
- $\Gamma = 107 \pm 5\ \text{MeV}/c^2$

$a_2{}'$ parameters

- $m = 1740\text{–}1890\ \text{MeV}/c^2$
- $\Gamma = 300\text{–}555\ \text{MeV}/c^2$

cf. PDG 2012 “omitted from summary”: $a_2(1700)$

- $m = 1732 \pm 16\ \text{MeV}/c^2$
- $\Gamma = 194 \pm 40\ \text{MeV}/c^2$

PWA of $\pi^- p \to \pi^-\pi^+\pi^- p_{\text{recoil}}$: Fit of Mass Dependence

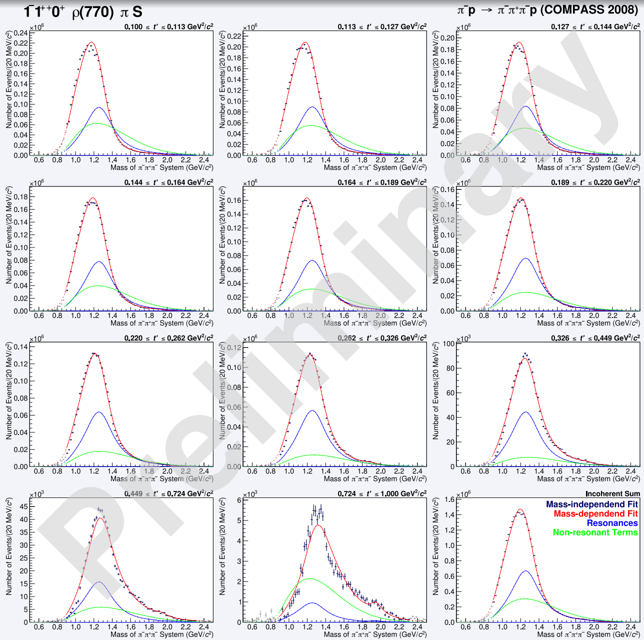

$1^{++}\,0^{+}\,\rho\pi S$

$a_1(1260)$ parameters

- $m = 1260\text{-}1290\ \text{MeV}/c^2$
- $\Gamma = 360\text{-}420\ \text{MeV}/c^2$

Cf. PDG 2012

- $m = 1230 \pm 40\ \text{MeV}/c^2$
- $\Gamma = 250\text{-}400\ \text{MeV}/c^2$

$a_1{}'$ parameters

- $m = 1920\text{–}2000\ \text{MeV}/c^2$
- $\Gamma = 155\text{–}255\ \text{MeV}/c^2$

cf. PDG 2012 “further states”: $a_1(1930)$

- $m = 1930^{+30}_{-70}\ \text{MeV}/c^2$
- $\Gamma = 155 \pm 45\ \text{MeV}/c^2$

PWA of $\pi^- p \to \pi^-\pi^+\pi^- p_{\text{recoil}}$: Fit of Mass Dependence

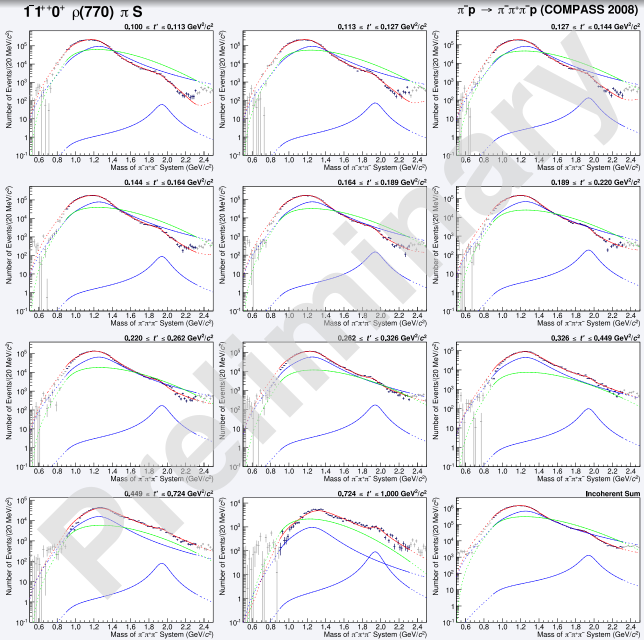

$1^{++}\,0^+\,\rho\pi S$

$a_1(1260)$ parameters

- $m = 1260\text{-}1290\ \text{MeV}/c^2$
- $\Gamma = 360\text{-}420\ \text{MeV}/c^2$

Cf. PDG 2012

- $m = 1230 \pm 40\ \text{MeV}/c^2$
- $\Gamma = 250\text{-}400\ \text{MeV}/c^2$

$a_1{}'$ parameters

- $m = 1920\text{–}2000\ \text{MeV}/c^2$
- $\Gamma = 155\text{–}255\ \text{MeV}/c^2$

cf. PDG 2012 “further states”: $a_1(1930)$

- $m = 1930^{+30}_{-70}\ \text{MeV}/c^2$
- $\Gamma = 155 \pm 45\ \text{MeV}/c^2$

PWA of $\pi^- p \to \pi^- \pi^+ \pi^- p_{\text{recoil}}$: Fit of Mass Dependence

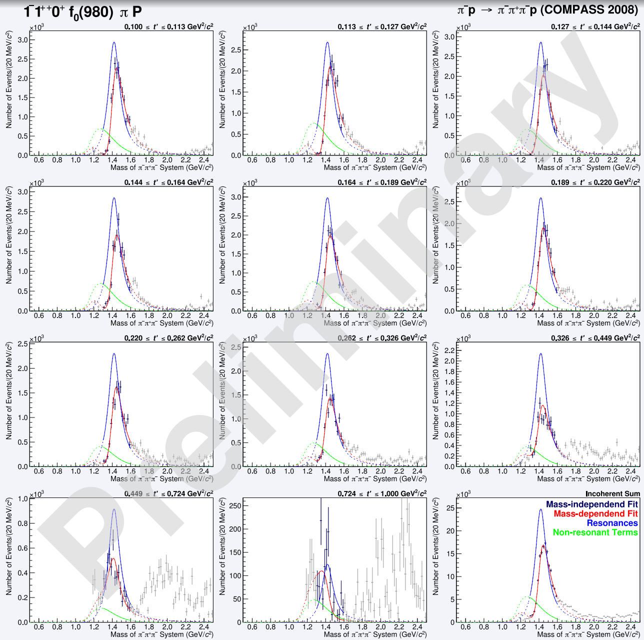

$1^{++}\,0^+\,f_0(980)\pi P$

$a_1(1420)$ parameters

- $m = 1412\text{-}1422$ MeV/c^2
- $\Gamma = 130\text{-}150$ MeV/c^2

Not in PDG

PWA of $\pi^- p \to \pi^-\pi^+\pi^- p_{\text{recoil}}$: Fit of Mass Dependence

Relative Phases of $1^{++}\,0^+\,f_0(980)\pi P$ Partial Wave

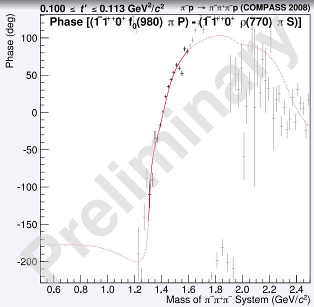

Significant phase motion w.r.t.

- $1^{++}\,0^+\,\rho\pi S$
- $2^{++}\,1^+\,\rho\pi D$
- $2^{-+}\,0^+\,f_2\pi S$
- $4^{++}\,1^+\,\rho\pi G$

Consistent with Breit-Wigner resonance

PWA of $\pi^- p \to \pi^-\pi^+\pi^- p_{\text{recoil}}$: Fit of Mass Dependence

Relative Phases of $1^{++}\,0^+\,f_0(980)\pi P$ Partial Wave

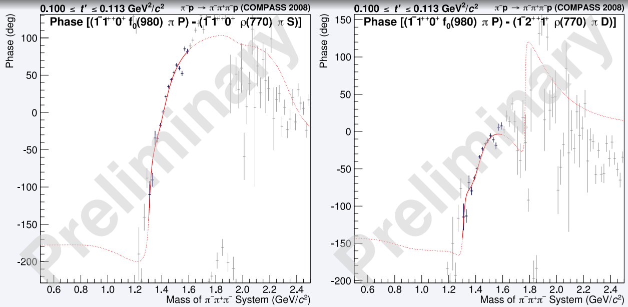

Significant phase motion w.r.t.

- $1^{++}\,0^+\,\rho\pi S$
- $2^{++}\,1^+\,\rho\pi D$
- $2^{-+}\,0^+\,f_2\pi S$
- $4^{++}\,1^+\,\rho\pi G$

Consistent with Breit-Wigner resonance

PWA of $\pi^- p \to \pi^-\pi^+\pi^- p_{\text{recoil}}$: Fit of Mass Dependence

Relative Phases of $1^{++}\,0^+\,f_0(980)\pi P$ Partial Wave

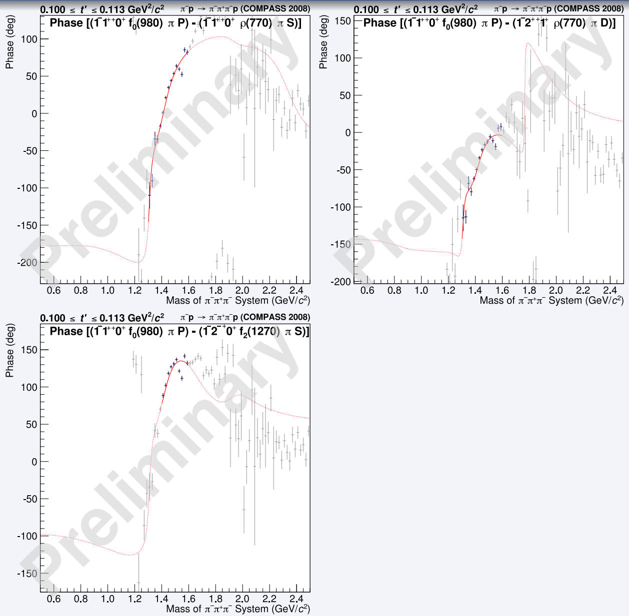

Significant phase motion w.r.t.

- $1^{++}\,0^+\,\rho\pi S$
- $2^{++}\,1^+\,\rho\pi D$
- $2^{-+}\,0^+\,f_2\pi S$
- $4^{++}\,1^+\,\rho\pi G$

Consistent with Breit-Wigner resonance

PWA of $\pi^- p \to \pi^-\pi^+\pi^- p_{\text{recoil}}$: Fit of Mass Dependence

Relative Phases of $1^{++}\,0^+\,f_0(980)\pi P$ Partial Wave

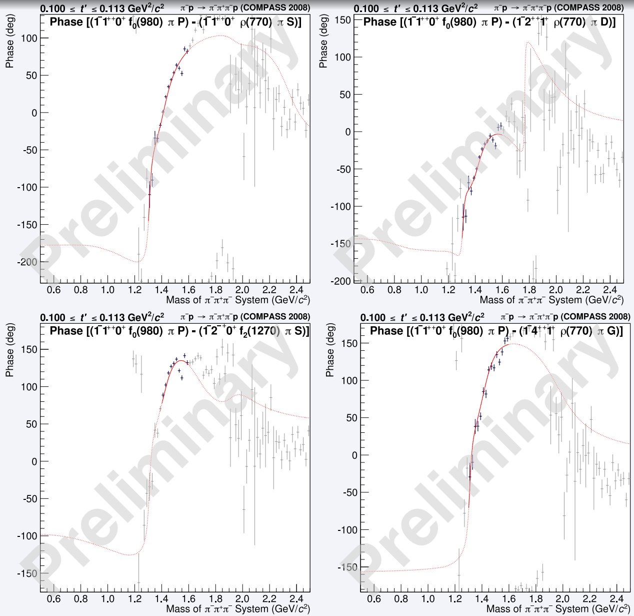

Significant phase motion w.r.t.

- $1^{++}\,0^+\,\rho\pi S$
- $2^{++}\,1^+\,\rho\pi D$
- $2^{-+}\,0^+\,f_2\pi S$
- $4^{++}\,1^+\,\rho\pi G$

Consistent with Breit-Wigner resonance

PWA of $\pi^- p \to \pi^-\pi^+\pi^- p_{\mathrm{recoil}}$: Fit of Mass Dependence

Relative Phases of $1^{++}\,0^+\,f_0(980)\pi P$ Partial Wave

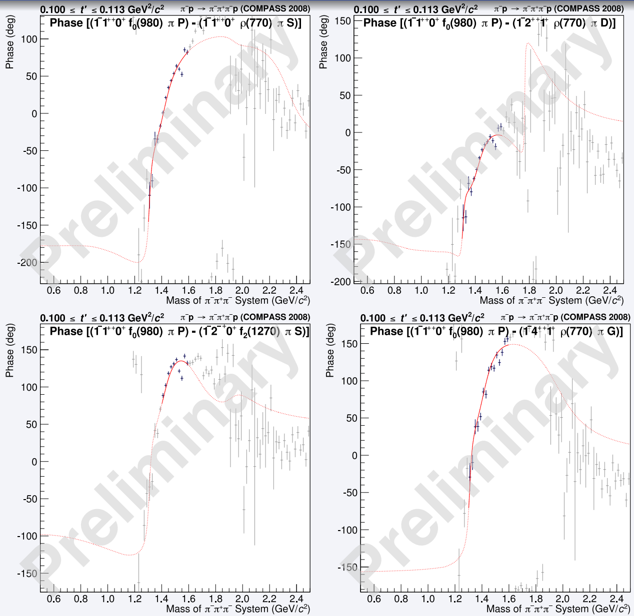

Significant phase motion w.r.t.

- $1^{++}\,0^+\,\rho\pi S$
- $2^{++}\,1^+\,\rho\pi D$
- $2^{-+}\,0^+\,f_2\pi S$
- $4^{++}\,1^+\,\rho\pi G$

Consistent with Breit-Wigner resonance

Outline

1. Introduction
   - QCD and the constituent quark model
   - Beyond the constituent quark model
2. How to measure meson spectra?
   - Meson production in diffractive dissociation
   - Partial-wave analysis method
3. Selected results
   - Partial-wave decomposition of the $(3\pi)^-$ final state
   - Resonance extraction in the $\pi^-\pi^+\pi^-$ system
4. Conclusions and outlook

Conclusions and Outlook

World's largest $\pi^-\pi^+\pi^-$ data set

- Crosscheck systematics with $\pi^-\pi^0\pi^0$ data
- *Novel analysis scheme:* binning in t'
  - Better separation of resonant and non-resonant contribution
- Determination of resonance parameters still work in progress
  - Limited by systematics
  - Improved models needed
    - Better parametrization of non-resonant contribution
  - *Future:* include more partial waves in mass-dependent fit
    - Better contraint parameters of excited states
    - Extraction of branching fractions

Conclusions and Outlook

New state $a_1(1420)$ seen in $f_0(980)\pi$ decay mode

- $m = 1412\text{-}1422\ \mathrm{MeV}/c^2$, $\Gamma = 130\text{-}150\ \mathrm{MeV}/c^2$
- No quark-model states expected in this mass region
- Pronounced phase motion w.r.t. to other waves

Nature of $a_1(1420)$ still unclear

- Close to $K^*(892)\,\bar{K}$ threshold
- Isospin partner of $f_1(1420)$?
- Coupled-channel effect with $a_1(1260) \to K^*(892)\,\bar{K} \to f_0(980)\,\pi$?
- …?

Broad intensity bump in spin-exotic $1^{-+}\,1^+\,\rho\pi P$ wave

- Resonance interpretation work in progress

Conclusions and Outlook

New state $a_1(1420)$ seen in $f_0(980)\pi$ decay mode

- $m = 1412\text{-}1422\ \text{MeV}/c^2$, $\Gamma = 130\text{-}150\ \text{MeV}/c^2$
- No quark-model states expected in this mass region
- Pronounced phase motion w.r.t. to other waves

Nature of $a_1(1420)$ still unclear

- Close to $K^*(892)\,\bar{K}$ threshold
- Isospin partner of $f_1(1420)$?
- Coupled-channel effect with $a_1(1260) \to K^*(892)\,\bar{K} \to f_0(980)\,\pi$?
- …?

Broad intensity bump in spin-exotic $1^{-+}\,1^+\,\rho\pi P$ wave

- Resonance interpretation work in progress

Conclusions and Outlook

New state $a_1(1420)$ seen in $f_0(980)\pi$ decay mode

- $m = 1412\text{-}1422\ \text{MeV}/c^2$, $\Gamma = 130\text{-}150\ \text{MeV}/c^2$
- No quark-model states expected in this mass region
- Pronounced phase motion w.r.t. to other waves

Nature of $a_1(1420)$ still unclear

- Close to $K^*(892)\,\bar{K}$ threshold
- Isospin partner of $f_1(1420)$?
- Coupled-channel effect with $a_1(1260) \to K^*(892)\,\bar{K} \to f_0(980)\,\pi$?
- …?

Broad intensity bump in spin-exotic $1^{-+}\,1^+\,\rho\pi P$ wave

- Resonance interpretation work in progress

But wait... There's More!

Other diffractively produced channels

- Pion beam: $\pi^-\eta$, $\pi^-\eta'$, $\pi^-\eta\eta$, $\pi^-\pi^0\omega$, $K\bar{K}\pi$, $K\bar{K}\pi\pi$, $\pi^-\pi^+\pi^-\pi^+\pi^-$, ...
- Kaon beam: $K^-\pi^+\pi^-$

Other production reactions

- Central production reactions
  - Study isoscalar $J^{PC} = 0^{++}$ mesons
- Diffractive production of baryon resonances
  - "Pomeron-induced"
  - E.g. $p\,p \to p\pi^+\pi^-\,p_{\text{recoil}}$

COMPASS is a unique experiment to study **light-quark hadron spectroscopy**

But wait... There's More!

Other diffractively produced channels

- Pion beam: $\pi^-\eta$, $\pi^-\eta'$, $\pi^-\eta\eta$, $\pi^-\pi^0\omega$, $K\bar{K}\pi$, $K\bar{K}\pi\pi$, $\pi^-\pi^+\pi^-\pi^+\pi^-$, ...
- Kaon beam: $K^-\pi^+\pi^-$

Other production reactions

- Central production reactions
  - Study isoscalar $J^{PC} = 0^{++}$ mesons
- Diffractive production of baryon resonances
  - "Pomeron-induced"
  - E.g. $p\,p \to p\pi^+\pi^-\,p_{\mathrm{recoil}}$

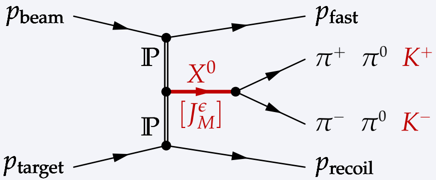

K^+K^- invariant mass

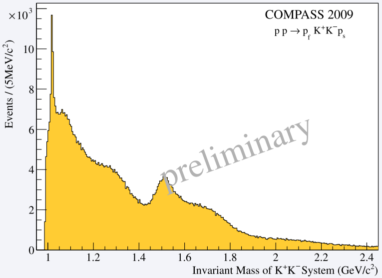

COMPASS is a unique experiment to study **light-quark hadron spectroscopy**

But wait. . . There's More!

Other diffractively produced channels

- Pion beam: $\pi^-\eta$, $\pi^-\eta'$, $\pi^-\eta\eta$, $\pi^-\pi^0\omega$, $K\bar{K}\pi$, $K\bar{K}\pi\pi$, $\pi^-\pi^+\pi^-\pi^+\pi^-$, ...
- Kaon beam: $K^-\pi^+\pi^-$

Other production reactions

- Central production reactions
  - Study isoscalar $J^{PC} = 0^{++}$ mesons
- Diffractive production of baryon resonances
  - "Pomeron-induced"
  - E.g. $p\,p \to p\pi^+\pi^-\,p_{\text{recoil}}$

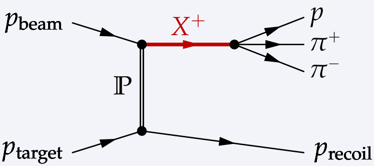

$50 \cdot 10^6\ p\pi^+\pi^-$ events

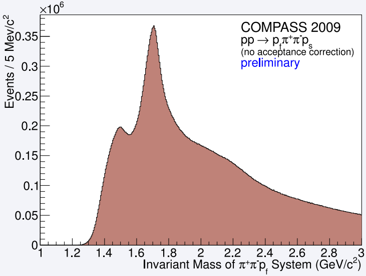

COMPASS is a unique experiment to study **light-quark hadron spectroscopy**

But wait. . . There's More!

Other diffractively produced channels

- Pion beam: $\pi^-\eta$, $\pi^-\eta'$, $\pi^-\eta\eta$, $\pi^-\pi^0\omega$, $K\bar{K}\pi$, $K\bar{K}\pi\pi$, $\pi^-\pi^+\pi^-\pi^+\pi^-$, ...
- Kaon beam: $K^-\pi^+\pi^-$

Other production reactions

- Central production reactions
  - Study isoscalar $J^{PC} = 0^{++}$ mesons
- Diffractive production of baryon resonances
  - "Pomeron-induced"
  - E.g. $p\,p \to p\pi^+\pi^-\,p_{\mathrm{recoil}}$

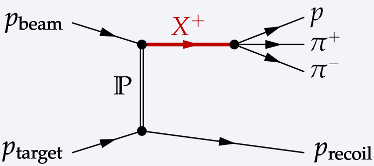

$50 \cdot 10^6$ $p\pi^+\pi^-$ events

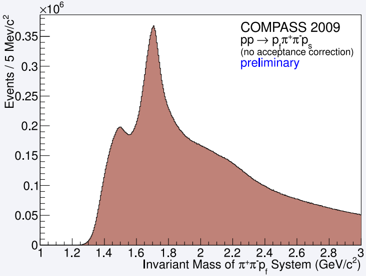

COMPASS is a unique experiment to study
light-quark hadron spectroscopy

Outline

5. Backup slides
   - Partial-wave analysis method
   - Partial-wave decomposition of $(3\pi)^-$ final states
   - Extraction of $[\pi\pi]_{S-wave}$ amplitude from $\pi^-\pi^+\pi^-$ system
   - Mass-dependent fit

Partial-Wave Analysis: The Basic Idea

Simplest case: **elastic scattering of non-relativistic spinless particles from static central potential**

J. J. Sakurai, "Modern QM" ch. 7.6

- Differential cross section from scattering amplitude f using transition operator T

$$\frac{\mathrm{d}\sigma}{\mathrm{d}\Omega} = |f(\vec{k},\vec{k}')|^2 \text{ with } f(\vec{k},\vec{k}') \propto \langle \vec{k}' | T | \vec{k} \rangle$$

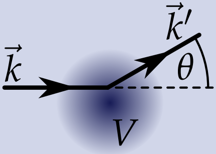

- Insert complete set $\{|L\,M\rangle\}$ of orthonormal basis states (spherical waves)

Completeness: $\sum_{L\,M} |L\,M\rangle\langle L\,M| = \mathbb{1}$

$$\begin{aligned} f(\vec{k},\vec{k}') &\propto \langle \vec{k}' | \mathbb{1}\, T\, \mathbb{1} | \vec{k} \rangle \\ &\propto \sum_{L'\,M'} \sum_{L\,M} \underbrace{\langle \vec{k}' | L'\,M' \rangle}_{\propto Y_{L'}^{M'}(\vec{k}')} \underbrace{\langle L'\,M' | T | L\,M \rangle}_{\propto T_L(E)} \underbrace{\langle L\,M | \vec{k} \rangle}_{\propto Y_L^M(\vec{k})} \\ &\propto \sum_L (2L+1)\, T_L(E)\, P_L(\cos\theta) \end{aligned}$$

Partial-Wave Analysis: The Basic Idea

***Simplest case:* elastic scattering of non-relativistic spinless particles from static central potential**

J. J. Sakurai, "Modern QM" ch. 7.6

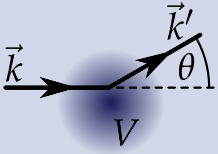

- Differential cross section from scattering amplitude f using transition operator T

  $\frac{\mathrm{d}\sigma}{\mathrm{d}\Omega} = |f(\vec{k},\vec{k}')|^2$ with $f(\vec{k},\vec{k}') \propto \langle\vec{k}'|T|\vec{k}\rangle$

- Insert complete set $\{|L\,M\rangle\}$ of orthonormal basis states (spherical waves)

  Completeness: $\sum_{L\,M} |L\,M\rangle\langle L\,M| = \mathbb{1}$

$$
\begin{aligned}
f(\vec{k},\vec{k}') &\propto \langle\vec{k}'|\mathbb{1}\,T\,\mathbb{1}|\vec{k}\rangle \\
&\propto \sum_{L'\,M'} \sum_{L\,M} \underbrace{\langle\vec{k}'|L'\,M'\rangle}_{\propto\, Y_{L'}^{M'}(\vec{k}')} \underbrace{\langle L'\,M'|T|L\,M\rangle}_{\propto\, T_L(E)} \underbrace{\langle L\,M|\vec{k}\rangle}_{\propto\, Y_L^M(\vec{k})} \\
&\propto \sum_L (2L+1)\,T_L(E)\,P_L(\cos\theta)
\end{aligned}
$$

Partial-Wave Analysis: The Basic Idea

Simplest case: **elastic scattering of non-relativistic spinless particles from a static central potential** (cont.)

J. J. Sakurai, "Modern QM" ch. 7.6

$$f(\vec{k}, \vec{k}') \propto \sum_L (2L+1)\, T_L(E)\, P_L(\cos\theta)$$

- *Key feature:* for each L, terms factorize into
  - Dynamic amplitude $T_L(E)$
  - Angular distribution $P_L(\cos\theta)$
- Transition amplitudes T_L contain interesting dynamics
- At fixed E: determination of T_L from data by decomposition of angular distributions in terms of P_L
- $T_L(E)$ usually parameterized by phase $\delta_L(E)$ and inelasticity $\eta_L(E)$:

$$T_L(E) \equiv \frac{\eta_L(E) e^{2\imath\delta_L(E)} - 1}{2\imath}$$

Partial-Wave Analysis: The Basic Idea

Simplest case: **elastic scattering of non-relativistic spinless particles from a static central potential** (cont.)

J. J. Sakurai, "Modern QM" ch. 7.6

- *Key feature:*
  - Dynami
  - Angula
- Transition a interesting
- At fixed E: data by dec distribution
- $T_L(E)$ usua $\delta_L(E)$ and i

$T_L(E)$

Legendre polynomials

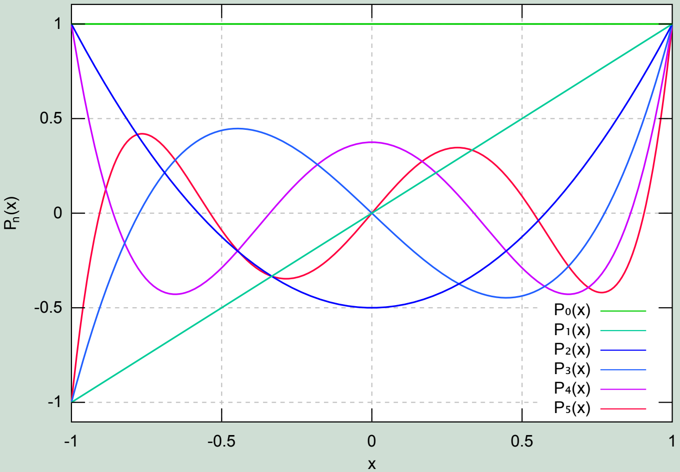

Partial-Wave Analysis: The Basic Idea

Simplest case: **elastic scattering of non-relativistic spinless particles from a static central potential** (cont.) J. J. Sakurai, "Modern QM" ch. 7.6

$$f(\vec{k}, \vec{k}') \propto \sum_L (2L+1)\, T_L(E)\, P_L(\cos\theta)$$

- *Key feature:* for each L, terms factorize into
  - Dynamic amplitude $T_L(E)$
  - Angular distribution $P_L(\cos\theta)$
- Transition amplitudes T_L contain interesting dynamics
- At fixed E: determination of T_L from data by decomposition of angular distributions in terms of P_L
- $T_L(E)$ usually parameterized by phase $\delta_L(E)$ and inelasticity $\eta_L(E)$:

$$T_L(E) \equiv \frac{\eta_L(E) e^{2\imath\delta_L(E)} - 1}{2\imath}$$

Partial-Wave Analysis: The Basic Idea

Simplest case: **elastic scattering of non-relativistic spinless particles from a static central potential** (cont.)

J. J. Sakurai, "Modern QM" ch. 7.6

$$f(\vec{k},\vec{k}') \propto \sum_L (2L+1)\, T_L(E)\, P_L(\cos\theta)$$

- *Key feature:* for each L, terms factorize into
  - Dynamic amplitude $T_L(E)$
  - Angular distribution $P_L(\cos\theta)$
- Transition amplitudes T_L contain interesting dynamics
- At fixed E: determination of T_L from data by decomposition of angular distributions in terms of P_L
- $T_L(E)$ usually parameterized by phase $\delta_L(E)$ and inelasticity $\eta_L(E)$:

$$T_L(E) \equiv \frac{\eta_L(E)e^{2\imath\delta_L(E)} - 1}{2\imath}$$

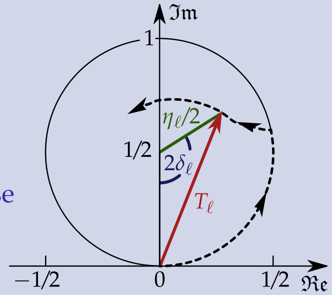

Reflectivity basis

S. U. Chung and T. L. Trueman, Phys. Rev. **D11** (1975) 633

- Reaction: beam + target $\rightarrow X$ + recoil
- Reflectivity operator Π_y: reflection through production plane
- Particles in production plane: Π_y acts like parity but leaves momenta unchanged
- Eigenstates to Π_y:
  $|J^P M^\epsilon\rangle \equiv c(M)\left[|J^P M\rangle - \epsilon\, P\,(-)^{J-M}|J^P\, {-M}\rangle\right]$ where $M \geq 0$ and
  $$c = \begin{cases} \frac{1}{2} & \text{for } M = 0, \\ \frac{1}{\sqrt{2}} & \text{for } M > 1 \end{cases}$$
- Reflectivity $\epsilon = \pm 1$ (for bosons)
- **Parity conservation:** amplitudes with different ϵ do *not* interfere
- ϵ corresponds to naturality of exchanged Reggeon
  - Pomeron has positive naturality $\implies$ $\epsilon = +1$ amplitudes dominant

Partial-Wave Analysis Formalism

Parity Conservation at Production Vertex

Reflectivity basis S. U. Chung and T. L. Trueman, Phys. Rev. **D11** (1975) 633

- Reaction: beam + target $\to X +$ recoil
- Reflectivity operator Π_y: reflection through production plane
- Particles in production plane: Π_y acts like parity but leaves momenta unchanged
- Eigenstates to Π_y:
  $|J^P M^\epsilon\rangle \equiv c(M)\left[|J^P M\rangle - \epsilon\, P\,(-)^{J-M}|J^P\, {-M}\rangle\right]$ where $M \geq 0$ and
  $$c = \begin{cases} \frac{1}{2} & \text{for } M = 0, \\ \frac{1}{\sqrt{2}} & \text{for } M > 1 \end{cases}$$
- Reflectivity $\epsilon = \pm 1$ (for bosons)
- **Parity conservation:** amplitudes with different ϵ do *not* interfere
- ϵ corresponds to naturality of exchanged Reggeon
  - Pomeron has positive naturality $\implies$ $\epsilon = +1$ amplitudes dominant

Reflectivity basis

S. U. Chung and T. L. Trueman, Phys. Rev. **D11** (1975) 633

- Reaction: beam + target $\to X +$ recoil
- Reflectivity operator Π_y: reflection through production plane
- Particles in production plane: Π_y acts like parity but leaves momenta unchanged
- Eigenstates to Π_y:
  $|J^P M^\epsilon\rangle \equiv c(M)\left[|J^P M\rangle - \epsilon\, P\, (-)^{J-M}|J^P\, {-M}\rangle\right]$ where $M \geq 0$ and
  $$c = \begin{cases} \frac{1}{2} & \text{for } M = 0, \\ \frac{1}{\sqrt{2}} & \text{for } M > 1 \end{cases}$$
- Reflectivity $\epsilon = \pm 1$ (for bosons)
- **Parity conservation:** amplitudes with different ϵ do *not* interfere
- ϵ corresponds to naturality of exchanged Reggeon
  - Pomeron has positive naturality $\implies \epsilon = +1$ amplitudes dominant

Two-body decay $a \to b + c$

- Kinematics defined by
  - Invariant mass m_a of a
  - Polar angles (θ, ϕ) of daughter b in rest frame of a
- Spin states of b and c are described in helicity basis
- J_b and J_c couple to total spin S
- Relative orbital angular momentum L between b and c
- L and S couple to J_a

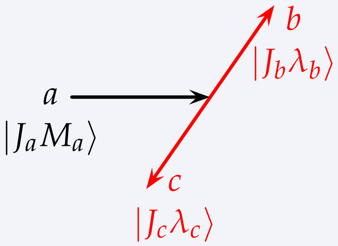

Partial-Wave Analysis Formalism

Decay Amplitude in the Helicity Formalism

Two-body decay $a \to b + c$

- Kinematics defined by
  - Invariant mass m_a of a
  - Polar angles (θ, ϕ) of daughter b in rest frame of a
- Spin states of b and c are described in helicity basis
- J_b and J_c couple to total spin S
- Relative orbital angular momentum L between b and c
- L and S couple to J_a

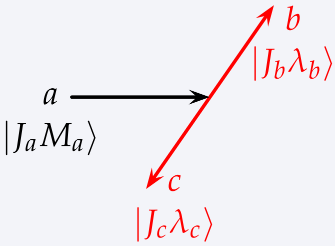

Two-body decay amplitude for $a \to b + c$

$$A_a(m_a, \theta, \phi) = \sqrt{2L+1} \sum_{\lambda_b, \lambda_c} (J_b\, \lambda_b\, J_c\, {-\lambda_c} | S\, \delta)\, (L\, 0\, S\, \delta | J_a\, \delta)$$
$$D^{J_a *}_{M_a \delta}(\theta, \phi, 0)\, F_L(q)\, \Delta(m_a)\, A_b\, A_c$$

Decay amplitude has no free parameters!

$\delta \equiv \lambda_b - \lambda_c$

$D^{J_a *}_{M_a \delta}(\theta, \phi, 0)$ D-function which describes rotation of helicity state

$F_L(q)$ Blatt-Weisskopf barrier factor for $a \to b\,[L]\,c$

q Breakup momentum for $a \to b + c$

$\Delta(m_a)$ Amplitude that describes resonance shape of a

$A_{b,c}$ decay amplitudes of (unstable) daughters b and c

Partial-Wave Analysis Formalism

Decay Amplitude in the Helicity Formalism

Two-body decay amplitude for $a \to b + c$

$$A_a(m_a, \theta, \phi) = \sqrt{2L+1} \sum_{\lambda_b, \lambda_c} (J_b\, \lambda_b\; J_c\, {-\lambda_c} | S\, \delta)\, (L\, 0\; S\, \delta | J_a\, \delta)$$
$$D^{J_a *}_{M_a \delta}(\theta, \phi, 0)\, F_L(q)\, \Delta(m_a)\, A_b\, A_c$$

Decay amplitude for multi-body final state

- Recursive calculation of two-body decay amplitudes for each vertex in isobar decay tree
- E.g. 2 vertices in $\pi^-\pi^+\pi^-$ case
  - X^- decay: Gottfried-Jackson frame
    - $\Delta(m_X) \equiv 1$
  - Isobar decay: helicity frame
  - $A_{\pi^\pm} \equiv 1$

Two-body decay amplitude for $a \to b + c$

$$A_a(m_a, \theta, \phi) = \sqrt{2L+1} \sum_{\lambda_b, \lambda_c} (J_b\, \lambda_b\; J_c\, {-\lambda_c} | S\, \delta)\, (L\, 0\; S\, \delta | J_a\, \delta)$$
$$D^{J_a *}_{M_a \delta}(\theta, \phi, 0)\, F_L(q)\, \Delta(m_a)\, A_b\, A_c$$

Decay amplitude for multi-body final state

- Recursive calculation of two-body decay amplitudes for each vertex in isobar decay tree
- E.g. 2 vertices in $\pi^-\pi^+\pi^-$ case
  - X^- decay: Gottfried-Jackson frame
    - $\Delta(m_X) \equiv 1$
  - Isobar decay: helicity frame
  - $A_{\pi^\pm} \equiv 1$

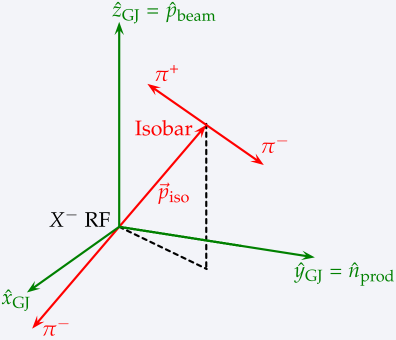

Partial-Wave Analysis Formalism

Decay Amplitude in the Helicity Formalism

Two-body decay amplitude for $a \to b + c$

$$A_a(m_a, \theta, \phi) = \sqrt{2L+1} \sum_{\lambda_b, \lambda_c} (J_b\, \lambda_b\, J_c\, {-\lambda_c} | S\, \delta)\, (L\, 0\, S\, \delta | J_a\, \delta)$$
$$D^{J_a *}_{M_a \delta}(\theta, \phi, 0)\, F_L(q)\, \Delta(m_a)\, A_b\, A_c$$

Decay amplitude for multi-body final state

- Recursive calculation of two-body decay amplitudes for each vertex in isobar decay tree
- E.g. 2 vertices in $\pi^-\pi^+\pi^-$ case
  - X^- decay: Gottfried-Jackson frame
    - $\Delta(m_X) \equiv 1$
  - Isobar decay: helicity frame
  - $A_{\pi^\pm} \equiv 1$

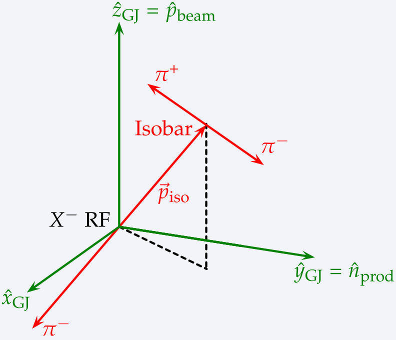

Two-body decay amplitude for $a \to b + c$

$$A_a(m_a, \theta, \phi) = \sqrt{2L+1} \sum_{\lambda_b, \lambda_c} (J_b\, \lambda_b\, J_c\, {-\lambda_c} | S\, \delta)\, (L\, 0\, S\, \delta | J_a\, \delta)$$

$$D^{J_a *}_{M_a \delta}(\theta, \phi, 0)\, F_L(q)\, \Delta(m_a)\, A_b\, A_c$$

Decay amplitude for multi-body final state

- Recursive calculation of two-body decay amplitudes for each vertex in isobar decay tree
- E.g. 2 vertices in $\pi^-\pi^+\pi^-$ case
  - X^- decay: Gottfried-Jackson frame
    - $\Delta(m_X) \equiv 1$
  - Isobar decay: helicity frame
  - $A_{\pi^\pm} \equiv 1$

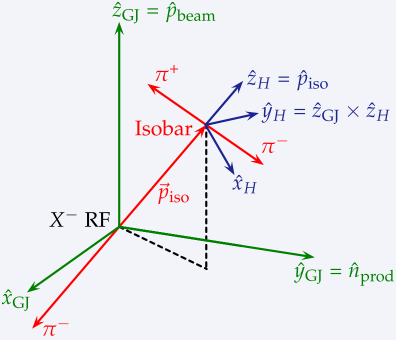

Partial-Wave Analysis Formalism

Cross section parameterization in mass-independent PWA

$$\mathcal{I}(\tau; m_X) = \sum_{\epsilon=\pm1} \sum_{r=1}^{\text{rank}} \left| \sum_{i}^{\text{waves}} T_i^{r\,\epsilon}(m_X)\, A_i^{\epsilon}(\tau) \right|^2$$

- ϵ, i: quantum numbers of partial wave ($J^{PC} M^{\epsilon}[\text{isobar}]L$)
- $T_i^{r\,\epsilon}$: complex production amplitudes; fit parameters
- A_i^{ϵ}: complex decay amplitudes
- τ: phase space coordinates

Spin-density matrix

$$\rho_{ij}^{\epsilon} = \sum_{r=1}^{\text{rank}} T_i^{r\,\epsilon}\, T_j^{r\,\epsilon *} \qquad \mathcal{I}(\tau; m_X) = \sum_{\epsilon=\pm1} \sum_{i,j}^{\text{waves}} \rho_{ij}^{\epsilon}(m_X)\, A_i^{\epsilon}(\tau)\, A_j^{\epsilon *}(\tau)$$

- Diagonal elements ρ_{ii}: intensities
- Off-diagonal elements ρ_{ii}, $i \neq j$: interference terms

Partial-Wave Analysis Formalism

Unbinned extended maximum likelihood fit in mass bins

- Likelihood $\mathcal{L}$ to observe N events distributed according to model cross section $\sigma(\tau; m_X)$ and detector acceptance $\mathrm{Acc}(\tau; m_X)$

$$\mathcal{L} = \underbrace{\left[\frac{\overline{N}^N}{N!} e^{-\overline{N}}\right]}_{\substack{\text{Poisson likelihood} \\ \text{to observe } N \text{ events}}} \prod_{k=1}^{N} \underbrace{\left[\frac{\sigma(\tau_k; m_X)\,\mathrm{Acc}(\tau_k; m_X)}{\int \mathrm{d}\Phi_n(\tau; m_X)\,\sigma(\tau; m_X)\,\mathrm{Acc}(\tau; m_X)}\right]}_{\text{likelihood to observe event } k}$$

- Expected nmb. of events $\overline{N} \propto \int \mathrm{d}\Phi_n(\tau; m_X)\,\sigma(\tau; m_X)\,\mathrm{Acc}(\tau; m_X)$
- n-body phase-space element $\mathrm{d}\Phi_n(\tau; m_X)$

Partial-Wave Analysis Formalism

Unbinned extended maximum likelihood fit in mass bins

- Likelihood $\mathcal{L}$ to observe N events distributed according to model cross section $\sigma(\tau; m_X)$ and detector acceptance $\mathrm{Acc}(\tau; m_X)$

$$\mathcal{L} = \underbrace{\left[\frac{\overline{N}^N}{N!} e^{-\overline{N}}\right]}_{\substack{\text{Poisson likelihood} \\ \text{to observe } N \text{ events}}} \prod_{k=1}^{N} \underbrace{\left[\frac{\sigma(\tau_k; m_X)\,\mathrm{Acc}(\tau_k; m_X)}{\int \mathrm{d}\Phi_n(\tau; m_X)\,\sigma(\tau; m_X)\,\mathrm{Acc}(\tau; m_X)}\right]}_{\text{likelihood to observe event } k}$$

- Expected nmb. of events $\overline{N} \propto \int \mathrm{d}\Phi_n(\tau; m_X)\,\sigma(\tau; m_X)\,\mathrm{Acc}(\tau; m_X)$
- n-body phase-space element $\mathrm{d}\Phi_n(\tau; m_X)$

Partial-Wave Analysis Formalism

Unbinned extended maximum likelihood fit in mass bins

- Insert intensity parameterization

$$\mathcal{I} = \sum_{\epsilon=\pm1} \sum_{r=1}^{\text{rank}} \left| \sum_{i}^{\text{waves}} T_i^{r\,\epsilon} A_i^{\epsilon} \right|^2$$

- Skip constant factors and take logarithm:

$$\ln \mathcal{L} = \sum_{k=1}^{N} \ln \left[\sum_{\epsilon=\pm1} \sum_{r=1}^{\text{rank}} \left| \sum_{i}^{\text{waves}} T_i^{r\,\epsilon} A_i^{\epsilon}(\tau_k) \right|^2 \right] - \sum_{\epsilon=\pm1} \sum_{r=1}^{\text{rank}} \sum_{i,j}^{\text{waves}} T_i^{r\,\epsilon} T_j^{r\,\epsilon *} \underbrace{\int \mathrm{d}\Phi_n(\tau)\, \mathrm{Acc}(\tau)\, A_i^{\epsilon}(\tau)\, A_j^{\epsilon *}(\tau)}_{\text{normalization integral } I_{ij}}$$

- Maximization of $\ln \mathcal{L}$ with $T_i^{r\,\epsilon}(m_X)$ as free parameters
- Decay amplitudes $A_i^{\epsilon}(\tau_k; m_X)$ are pre-calculated
- $I_{ij}(m_X)$ estimated using phase-space Monte Carlo

Partial-Wave Analysis Formalism

Unbinned extended maximum likelihood fit in mass bins

- Insert intensity parameterization

$$\mathcal{I} = \sum_{\epsilon=\pm1} \sum_{r=1}^{\text{rank}} \left| \sum_i^{\text{waves}} T_i^{r\,\epsilon} A_i^\epsilon \right|^2$$

- Skip constant factors and take logarithm:

$$\ln \mathcal{L} = \sum_{k=1}^{N} \ln \left[\sum_{\epsilon=\pm1} \sum_{r=1}^{\text{rank}} \left| \sum_i^{\text{waves}} T_i^{r\,\epsilon} A_i^\epsilon(\tau_k) \right|^2 \right]$$

$$- \sum_{\epsilon=\pm1} \sum_{r=1}^{\text{rank}} \sum_{i,j}^{\text{waves}} T_i^{r\,\epsilon} T_j^{r\,\epsilon*} \underbrace{\int \mathrm{d}\Phi_n(\tau)\,\mathrm{Acc}(\tau)\,A_i^\epsilon(\tau)\,A_j^{\epsilon*}(\tau)}_{\text{normalization integral } I_{ij}}$$

- Maximization of $\ln \mathcal{L}$ with $T_i^{r\,\epsilon}(m_X)$ as free parameters
- Decay amplitudes $A_i^\epsilon(\tau_k; m_X)$ are pre-calculated
- $I_{ij}(m_X)$ estimated using phase-space Monte Carlo

Partial-Wave Analysis: $\pi^-\pi^+\pi^-$ Final State

Test of fit quality

- Generate Monte-Carlo pseudodata according to model

$$\mathcal{I}(\tau; m_X) = \left| \sum_{\text{waves}} T_{\text{wave}}(m_X)\, A_{\text{wave}}(\tau; m_X) \right|^2$$

- Compare to real data

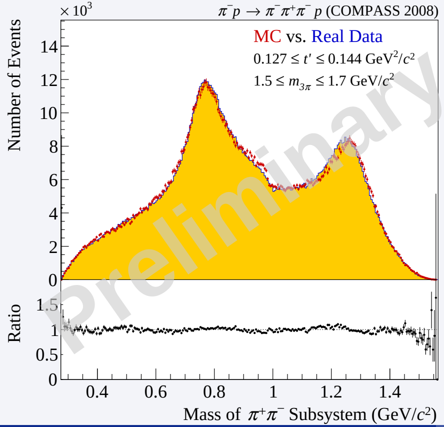

Example

- $m_{\pi^+\pi^-}$ distribution
  - $1.5 < m_{3\pi} < 1.7$ GeV$/c^2$
  - $0.127 < t' < 0.144$ (GeV$/c$)^2

Partial-Wave Analysis: $\pi^-\pi^+\pi^-$ Final State

Test of fit quality

- Generate Monte-Carlo pseudodata according to model

$$\mathcal{I}(\tau; m_X) = \left| \sum_{\text{waves}} T_{\text{wave}}(m_X)\, A_{\text{wave}}(\tau; m_X) \right|^2$$

- Compare to real data

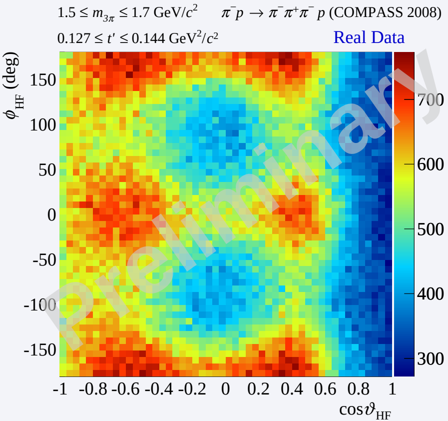

Example

- Angular distribution in isobar $\to \pi^+\pi^-$
  - $1.5 < m_{3\pi} < 1.7$ GeV/c^2
  - $0.127 < t' < 0.144$ $(\text{GeV}/c)^2$

Partial-Wave Analysis: $\pi^-\pi^+\pi^-$ Final State

Test of fit quality

- Generate Monte-Carlo pseudodata according to model

$$\mathcal{I}(\tau; m_X) = \left| \sum_{\text{waves}} T_{\text{wave}}(m_X)\, A_{\text{wave}}(\tau; m_X) \right|^2$$

- Compare to real data

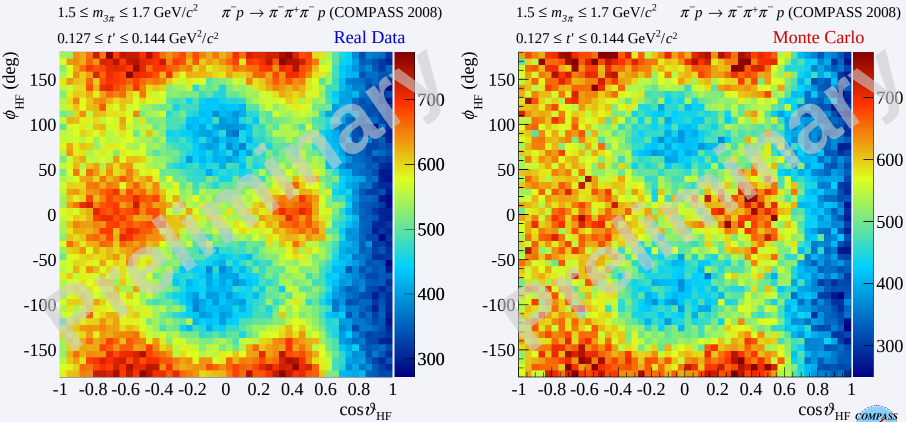

Partial-Wave Analysis: $\pi^-\pi^+\pi^-$ Final State

Test of fit quality

- Generate Monte-Carlo pseudodata according to model

$$\mathcal{I}(\tau; m_X) = \left| \sum_{\text{waves}} T_{\text{wave}}(m_X)\, A_{\text{wave}}(\tau; m_X) \right|^2$$

- Compare to real data

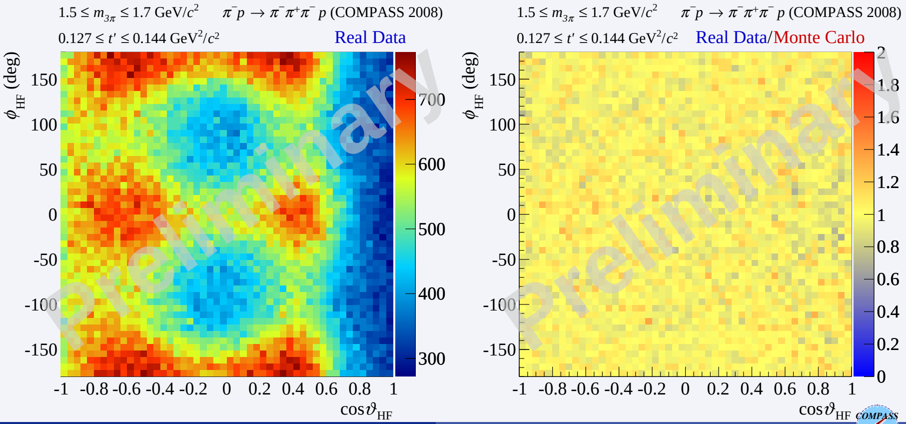

PWA of $\pi^- p \to (3\pi)^- p_{\text{recoil}}$: 6^{-+} Wave

Intensity of $6^{-+}0^+\rho\pi H$ Wave compared to Deck-Model (green)

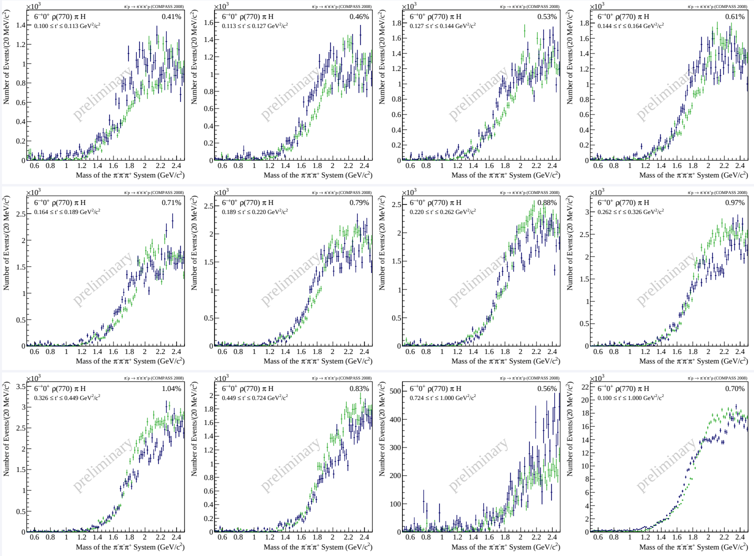

Deck intensity normalized to $6^{-+}1^+\rho\pi H$ t'-integrated intensity

PWA of $\pi^- p \to (3\pi)^- p_{\text{recoil}}$: 1^{-+} Spin-Exotic Wave

Intensity of $1^{-+}1^{+}\rho\pi P$ Wave compared to Deck-Model (green)

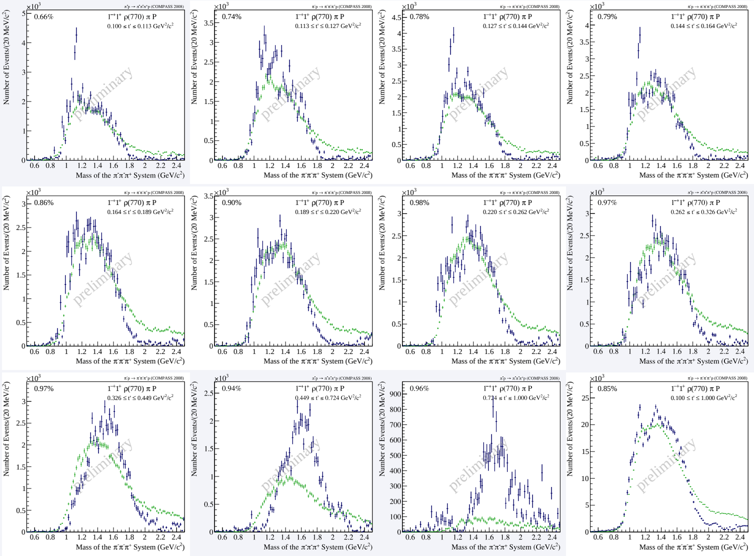

Deck intensity normalized to $1^{-+}1^{+}\rho\pi H$ t'-integrated intensity

PWA of $\pi^- p \to (3\pi)^- p_{\text{recoil}}$: 1^{-+} Spin-Exotic Wave

Relative Phases of $1^{-+}1^+\rho\pi P$ Wave

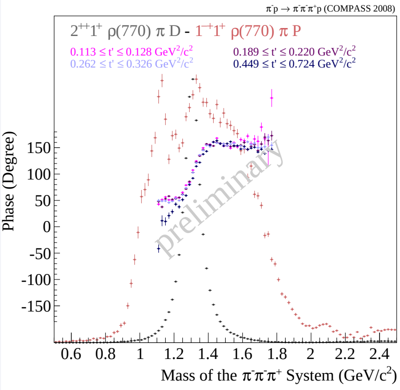

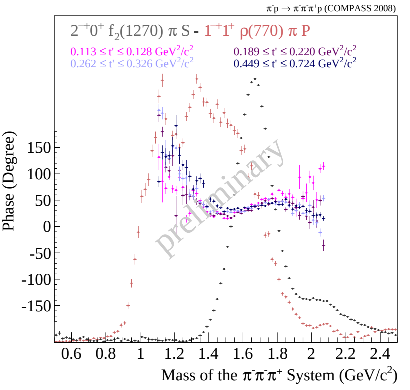

PWA of $\pi^- p \to (3\pi)^- p_{\text{recoil}}$: 1^{-+} Spin-Exotic Wave

Relative Phases of $1^{-+}1^+\rho\pi P$ Wave

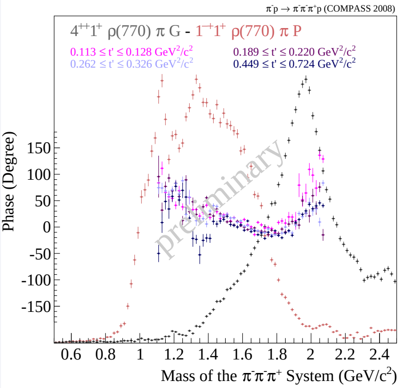

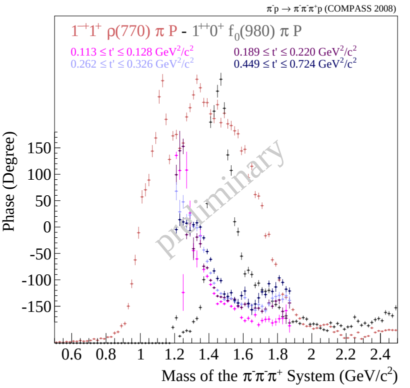

Is the $a_1(1420)$ a Model Artifact?

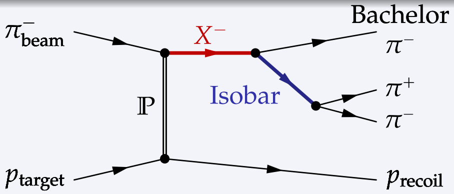

- PWA model

$$\mathcal{I}(\tau; m_X) = \left| \sum_{\text{waves}} T_{\text{wave}}(m_X)\, A_{\text{wave}}(\tau; m_X) \right|^2$$

- Decay amplitudes $A_{\text{wave}}(\tau)$
  - Need precise knowledge of isobar $\to \pi^+\pi^-$ amplitude
  - Parametrization of $J^{PC} = 0^{++}$ isobars difficult
    - $[\pi\pi]_{\text{S-wave}}$
    - $f_0(980)$
    - $f_0(1500)$
  - Information from $\pi\pi$ elastic scattering is used

Is the $a_1(1420)$ a Model Artifact?

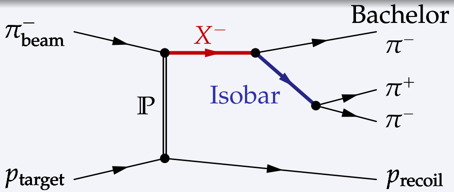

- PWA model

$$\mathcal{I}(\tau; m_X) = \left| \sum_{\text{waves}} T_{\text{wave}}(m_X)\, A_{\text{wave}}(\tau; m_X) \right|^2$$

- Decay amplitudes $A_{\text{wave}}(\tau)$
  - Need precise knowledge of isobar $\to \pi^+\pi^-$ amplitude
  - Parametrization of $J^{PC} = 0^{++}$ isobars difficult
    - $[\pi\pi]_{S\text{-wave}}$
    - $f_0(980)$
    - $f_0(1500)$
  - Information from $\pi\pi$ elastic scattering is used

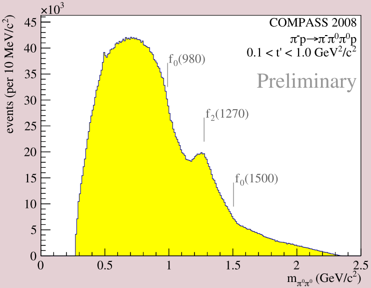

Is the $a_1(1420)$ a Model Artifact?

Novel analysis method

(inspired by E791, PRD **73** (2006) 032204)

- Replace $J^{PC} = 0^{++}$ isobar parametrizations by piece-wise constant amplitudes in $m_{\pi^+\pi^-}$ bins
- Extract $m_{3\pi}$ dependence of $J^{PC} = 0^{++}$ isobar amplitude from data
  - Drastic reduction of model bias
  - *Caveat:* significant increase in number of fit parameters

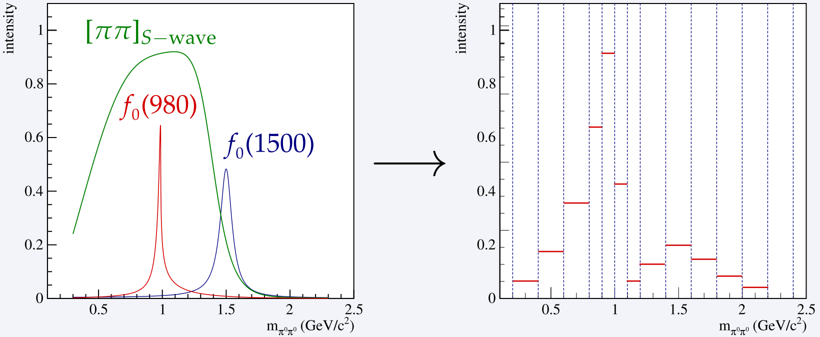

Is the $a_1(1420)$ a Model Artifact?

Novel analysis method

(inspired by E791, PRD **73** (2006) 032204)

- Replace $J^{PC} = 0^{++}$ isobar parametrizations by piece-wise constant amplitudes in $m_{\pi^+\pi^-}$ bins
- Extract $m_{3\pi}$ dependence of $J^{PC} = 0^{++}$ isobar amplitude from data
  - Drastic reduction of model bias
  - *Caveat:* significant increase in number of fit parameters

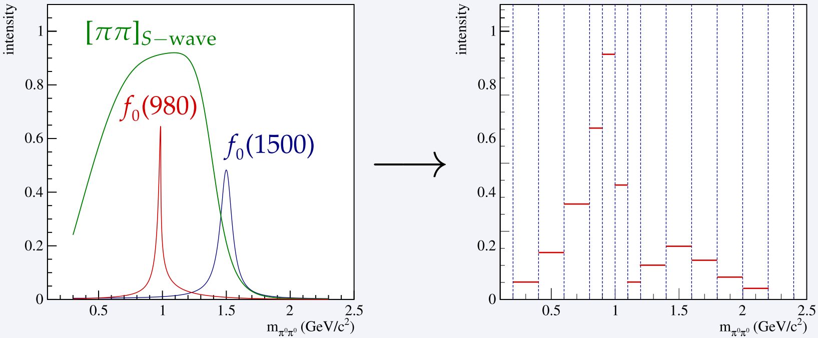

Extraction of $[\pi\pi]_{S\text{-wave}}$ from Data: $J^{PC} = 0^{-+}$ Wave

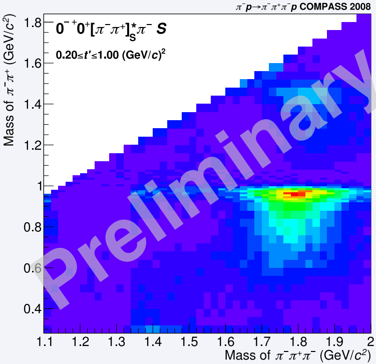

- Strong correlation of $\pi(1800)$ with $f_0(980)$
- Some signal for $\pi(1800) \to f_0(1500)\pi$

Extraction of $[\pi\pi]_{S\text{-wave}}$ from Data: $J^{PC} = 0^{-+}$ Wave

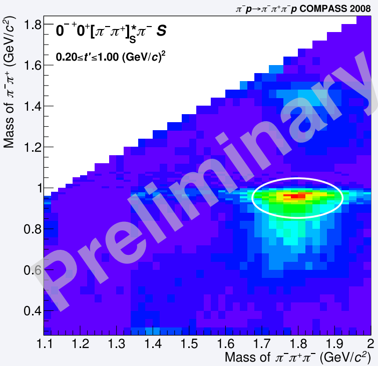

- Strong correlation of $\pi(1800)$ with $f_0(980)$
- Some signal for $\pi(1800) \to f_0(1500)\pi$

Extraction of $[\pi\pi]_{S\text{-wave}}$ from Data: $J^{PC} = 0^{-+}$ Wave

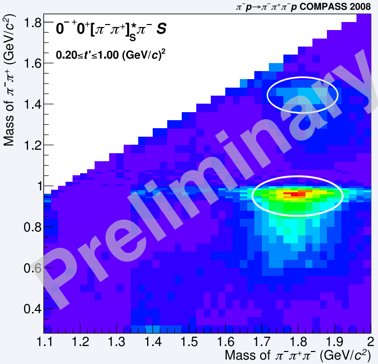

- Strong correlation of $\pi(1800)$ with $f_0(980)$
- Some signal for $\pi(1800) \to f_0(1500)\pi$

Extraction of $[\pi\pi]_{S\text{-wave}}$ from Data: $J^{PC} = 0^{-+}$ Wave

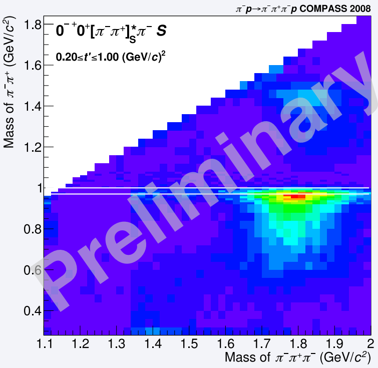

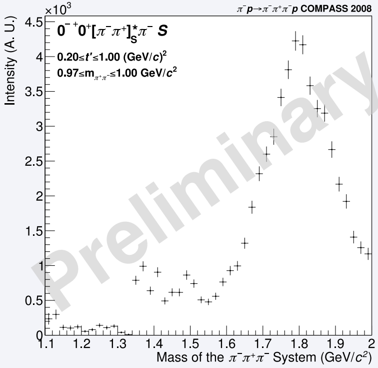

- Strong correlation of $\pi(1800)$ with $f_0(980)$
- Some signal for $\pi(1800) \to f_0(1500)\pi$

Extraction of $[\pi\pi]_{S\text{-wave}}$ from Data: $J^{PC} = 1^{++}$ Wave

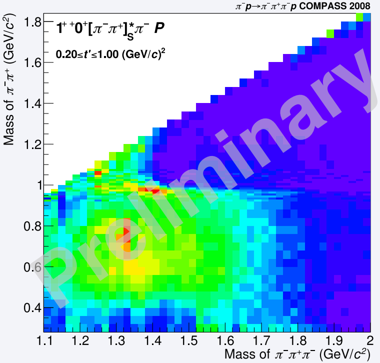

- Correlation of 3π intensity around 1.4 GeV/c^2 with $f_0(980)$
- Confirms that $a_1(1420)$ signal is *not* an artifact of isobar parametrization

Extraction of $[\pi\pi]_{S\text{-wave}}$ from Data: $J^{PC} = 1^{++}$ Wave

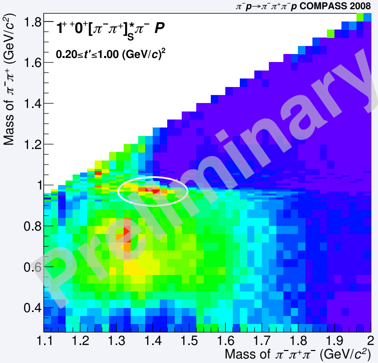

- Correlation of 3π intensity around 1.4 GeV/c^2 with $f_0(980)$
- Confirms that $a_1(1420)$ signal is *not* an artifact of isobar parametrization

Extraction of $[\pi\pi]_{S\text{-wave}}$ from Data: $J^{PC} = 1^{++}$ Wave

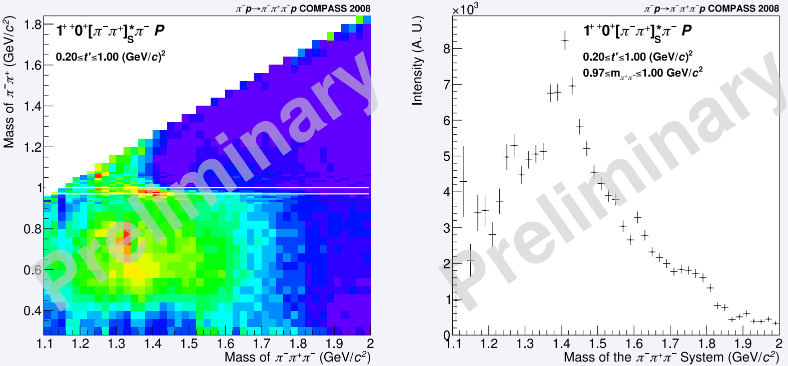

- Correlation of 3π intensity around 1.4 GeV/c^2 with $f_0(980)$
- Confirms that $a_1(1420)$ signal is *not* an artifact of isobar parametrization

Conclusions and Outlook

New method: extraction of $[\pi\pi]_{S\text{-wave}}$ amplitude from data

- Strong dependence on mother wave and $m_{3\pi}$
- Confirms coupling of $a_1(1420)$ to $f_0(980)\pi$
- *Future:*
    - Apply method to $[\pi\pi]$ P-, D-, F-, ... waves
    - Bootstrapping: put extracted isobar amplitudes back into fit
    - Parametrization of $[\pi\pi]_{S\text{-wave}}$ amplitude as function of $m_{3\pi}$
        - Extraction of isobar resonance parameters

Partial-Wave Analysis Formalism

Parametrization of Mass-Dependence of Spin-Density Matrix

Ansatz: $\rho_{ij}^{\epsilon}(m_X, t') = \sum_{r=1}^{\text{rank}} T_i^{r\,\epsilon}(m_X, t')\, T_j^{r\,\epsilon *}(m_X, t')$

$$T_i^{r\,\epsilon}(m_X, t') = \sum_{k_i}^{\text{resonances}} C_{irk}^{\epsilon}(t')\, \mathcal{A}_k(m_X; \zeta_k)\, \underbrace{\sqrt{\int \mathrm{d}\Phi_n(\tau)\, |A_i^{\epsilon}(\tau; m_X)|^2}}_{\text{phase space for wave } i}$$

Dynamic amplitudes $\mathcal{A}_k(m_X; \zeta_k)$

- Resonance line shapes
  - Typically relativistic Breit-Wigner with mass-dependent width

$$\mathcal{A}_k^{\text{BW}}(m_X; m_0, \Gamma_0) = \frac{m_0\, \Gamma_0}{m_0^2 - m_X^2 - i\, m_0\, \Gamma_{\text{tot}}(m_X)}$$

$$\Gamma_{\text{tot}}(m_X) = \sum_{\nu}^{\text{decays}} \Gamma_\nu(m_X) = \sum_{\nu}^{\text{decays}} \Gamma_{0,\nu}\, \frac{m_0}{m_X}\, \frac{q_\nu}{q_{0,\nu}}\, \frac{F_{L_\nu}(q_\nu)}{F_{L_\nu}(q_{0,\nu})}$$

- Non-resonant coherent background contributions
  - Typically exponentially damped phase space:
    $\mathcal{A}_k^{\text{BG}}(m_X; a_k) = e^{-a_k\, q_k^2}$

Partial-Wave Analysis Formalism

Parametrization of Mass-Dependence of Spin-Density Matrix

Ansatz: $\rho_{ij}^{\epsilon}(m_X, t') = \sum_{r=1}^{\text{rank}} T_i^{r\,\epsilon}(m_X, t')\, T_j^{r\,\epsilon *}(m_X, t')$

$$T_i^{r\,\epsilon}(m_X, t') = \sum_{k_i}^{\text{resonances}} C_{irk}^{\epsilon}(t')\, \mathcal{A}_k(m_X; \zeta_k) \underbrace{\sqrt{\int \mathrm{d}\Phi_n(\tau)\, |A_i^{\epsilon}(\tau; m_X)|^2}}_{\text{phase space for wave } i}$$

Dynamic amplitudes $\mathcal{A}_k(m_X; \zeta_k)$

- Resonance line shapes
  - Typically relativistic Breit-Wigner with mass-dependent width

$$\mathcal{A}_k^{\text{BW}}(m_X; m_0, \Gamma_0) = \frac{m_0\, \Gamma_0}{m_0^2 - m_X^2 - i\, m_0\, \Gamma_{\text{tot}}(m_X)}$$

$$\Gamma_{\text{tot}}(m_X) = \sum_{\nu}^{\text{decays}} \Gamma_\nu(m_X) = \sum_{\nu}^{\text{decays}} \Gamma_{0,\nu}\, \frac{m_0}{m_X}\, \frac{q_\nu}{q_{0,\nu}}\, \frac{F_{L_\nu}(q_\nu)}{F_{L_\nu}(q_{0,\nu})}$$

- Non-resonant coherent background contributions
  - Typically exponentially damped phase space:
    $\mathcal{A}_k^{\text{BG}}(m_X; a_k) = e^{-a_k q_k^2}$

Partial-Wave Analysis Formalism

Parametrization of Mass-Dependence of Spin-Density Matrix

Ansatz: $\rho_{ij}^{\epsilon}(m_X, t') = \sum_{r=1}^{\text{rank}} T_i^{r\,\epsilon}(m_X, t')\, T_j^{r\,\epsilon *}(m_X, t')$

$$T_i^{r\,\epsilon}(m_X, t') = \sum_{k_i}^{\text{resonances}} C_{irk}^{\epsilon}(t')\, \mathcal{A}_k(m_X; \zeta_k) \underbrace{\sqrt{\int \mathrm{d}\Phi_n(\tau)\, |A_i^{\epsilon}(\tau; m_X)|^2}}_{\text{phase space for wave } i}$$

Dynamic amplitudes $\mathcal{A}_k(m_X; \zeta_k)$

- Resonance line shapes
  - Typically relativistic Breit-Wigner with mass-dependent width

$$\mathcal{A}_k^{\text{BW}}(m_X; m_0, \Gamma_0) = \frac{m_0\, \Gamma_0}{m_0^2 - m_X^2 - i\, m_0\, \Gamma_{\text{tot}}(m_X)}$$

$$\Gamma_{\text{tot}}(m_X) = \sum_{\nu}^{\text{decays}} \Gamma_\nu(m_X) = \sum_{\nu}^{\text{decays}} \Gamma_{0,\nu}\, \frac{m_0}{m_X}\, \frac{q_\nu}{q_{0,\nu}}\, \frac{F_{L_\nu}(q_\nu)}{F_{L_\nu}(q_{0,\nu})}$$

- Non-resonant coherent background contributions
  - Typically exponentially damped phase space:
    $\mathcal{A}_k^{\text{BG}}(m_X; a_k) = e^{-a_k\, q_k^2}$

Partial-Wave Analysis Formalism

Parametrization of Mass-Dependence of Spin-Density Matrix

Ansatz: $\rho_{ij}^{\epsilon}(m_X, t') = \sum_{r=1}^{\text{rank}} T_i^{r\,\epsilon}(m_X, t')\, T_j^{r\,\epsilon *}(m_X, t')$

$$T_i^{r\,\epsilon}(m_X, t') = \sum_{k_i}^{\text{resonances}} C_{irk}^{\epsilon}(t')\, \mathcal{A}_k(m_X; \zeta_k) \sqrt{\underbrace{\int \mathrm{d}\Phi_n(\tau)\, |A_i^{\epsilon}(\tau; m_X)|^2}_{\text{phase space for wave } i}}$$

Model parameters determined by χ^2 fit to $\rho_{ij}^{\epsilon}(m_X)$

Free parameters:

- Complex amplitudes C_{irk}^{ϵ}
- Resonance or background parameters in $\mathcal{A}_k(m_X)$